AD-A160 262 CALIBRATION AND USE OF FIVE-HOLE FLOW DIRECTION PROBES FOR LOW SPEED WIND.. (U) NATIONAL AERONAUTICAL ESTABLISHMENT OTTAWA (ONTARIO) R H WICKENS ET AL. 1/1

UNCLASSIFIED JUL 85 NAE-AN-29 NRC-24468 F/G 14/2 NL

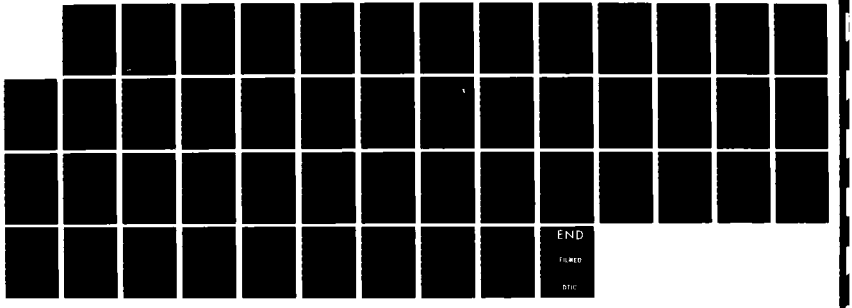

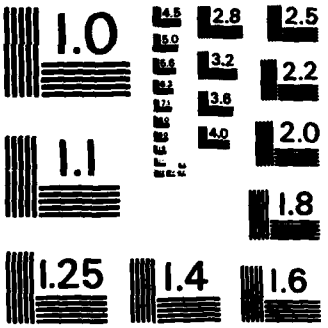

MICROCOPY RESOLUTION TEST CHART
NATIONAL BUREAU OF STANDARDS-1963-A

Canada

(6)

CALIBRATION AND USE OF FIVE-HOLE FLOW DIRECTION PROBES FOR LOW SPEED WIND TUNNEL APPLICATION

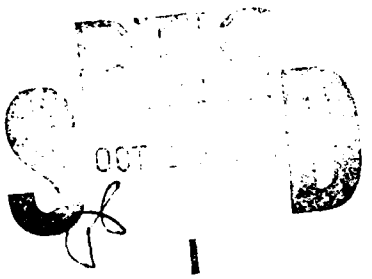

by

R.H. Wickens, C.D. Williams
National Aeronautical Establishment

AERONAUTICAL NOTE
NAE-AN-29
NRC NO. 24468

OTTAWA
JULY 1985

National Research Council Canada
Conseil national de recherches Canada

NATIONAL AERONAUTICAL ESTABLISHMENT

SCIENTIFIC AND TECHNICAL PUBLICATIONS

AERONAUTICAL REPORTS:

Aeronautical Reports (LR): Scientific and technical information pertaining to aeronautics considered important, complete, and a lasting contribution to existing knowledge.

Mechanical Engineering Reports (MS): Scientific and technical information pertaining to investigations outside aeronautics considered important, complete, and a lasting contribution to existing knowledge.

AERONAUTICAL NOTES (AN): Information less broad in scope but nevertheless of importance as a contribution to existing knowledge.

LABORATORY TECHNICAL REPORTS (LTR): Information receiving limited distribution because of preliminary data, security classification, proprietary, or other reasons.

Details on the availability of these publications may be obtained from:

Publications Section,
National Research Council Canada,
National Aeronautical Establishment,
Bldg. M-16, Room 204,
Montreal Road,
Ottawa, Ontario
K1A 0R6

ÉTABLISSEMENT AÉRONAUTIQUE NATIONAL

PUBLICATIONS SCIENTIFIQUES ET TECHNIQUES

RAPPORTS D'AÉRONAUTIQUE

Rapports d'aéronautique (LR): Informations scientifiques et techniques touchant l'aéronautique jugées importantes, complètes et durables en termes de contribution aux connaissances actuelles.

Rapports de génie mécanique (MS): Informations scientifiques et techniques sur la recherche externe à l'aéronautique jugées importantes, complètes et durables en termes de contribution aux connaissances actuelles.

CAHIERS D'AÉRONAUTIQUE (AN): Informations de moindre portée mais importantes en termes d'accroissement des connaissances.

RAPPORTS TECHNIQUES DE LABORATOIRE (LTR): Informations peu disséminées pour des raisons d'usage secret, de droit de propriété ou autres ou parce qu'elles constituent des données préliminaires.

Les publications ci-dessus peuvent être obtenues à l'adresse suivante:

Section des publications
Conseil national de recherches Canada
Établissement aéronautique national
Im. M-16, pièce 204
Chemin de Montréal
Ottawa (Ontario)
K1A 0R6

UNLIMITED
UNCLASSIFIED

CALIBRATION AND USE OF FIVE-HOLE FLOW DIRECTIONS PROBES FOR LOW SPEED WIND TUNNEL APPLICATION

ÉTALONNAGE ET EMPLOI DE CAPTEURS DE DIRECTION À CINQ TROUS EN SOUFFLERIE À BASSE VITESSE

by/par

R.H. Wickens, C.D. Williams

National Aeronautical Establishment

AERONAUTICAL NOTE
NAE-AN-29
NRC NO. 24468

OTTAWA
JULY 1985

R.J. Templin, Head/Chef
Low Speed Aerodynamics Laboratory/
Laboratoire d'aérodynamique à basse vitesse

G.M. Lindberg
Director/Directeur

SUMMARY

This note describes a method of calibration and use of five-hole flow direction probes. When used in complex three-dimensional mixed flows, the probe will furnish flow directions, velocity components and total pressures. The method described in this note is intended for the use of the wind tunnel project engineer in determining flow direction characteristics of various model configurations.

RÉSUMÉ

La présente note décrit une méthode d'étalonnage et l'emploi de sondes de direction à cinq trous. Utilisés dans des écoulements mixtes complexes à trois dimensions, ces sondes fournissent les directions, les composantes vitesses et les pressions totales des écoulements. La méthode décrite est destinée à l'ingénieur de soufflerie, pour lui permettre de déterminer les caractéristiques des directions des écoulements de divers profils.

CONTENTS

TABLES

ILLUSTRATIONS

ILLUSTRATIONS (Cont'd)

APPENDICES

SYMBOLS

Symbol	Definition
C_{pi}	probe orifice pressure coefficient (i = 1-5)
$\bar{C}_p$	average of four peripheral pressures
C_{ps}	local static pressure coefficient $C_{pt} - q/q_T$
C_{pt}	local total pressure coefficient $\frac{p_t - p_o}{1/2\,\rho V_T^2}$
p_o	tunnel reference pressure (wall static pressure)
p_T	tunnel total pressure
p_s	local static pressure
p_t	local total pressure
P	dynamic pressure parameter
Q	yaw-plane parameter
R	pitch-plane parameter
S	static pressure parameter

SYMBOLS (Cont'd)

Symbol	Definition
$S_{CAL}(\theta, \phi)$	empirical static pressure parameter
$P_{CAL}(\theta, \phi)$	empirical dynamic pressure parameter
V_R	resultant flow velocity
V_T	tunnel velocity
u,v,w	local flow components
q, q_T	local and tunnel dynamic pressure
θ	inclination of the flow vector in the combined pitch-yaw plane ($0 < \theta < +90°$)
ϕ	roll angle of the flow vector in the cross flow plane ($0 < \phi < 360°$) (measured clockwise from downward vertical axis)
α	pitch angle of the local flow, in the plane of orifices one and three
β	yaw angle of the local flow, in the plane of orifices two and four

CALIBRATION AND USE OF FIVE-HOLE FLOW DIRECTION PROBES FOR LOW SPEED WIND TUNNEL APPLICATION

1.0 INTRODUCTION

The five-hole flow direction probe is normally used to explore complex three-dimensional wakes which may be characterized by mixed regions of propulsive flow from jets or propeller slip-streams, and vortex flows, resulting from circulation-induced lift. These wakes are known to have a large variation of flow direction, flow velocity and total pressure, and it is convenient to be able to use a single probe which will measure alll of these quantities simultaneously, accurately, and without the necessity of nulling the individual side-hole pressures.

The probe configuration described in this report consists of five pressure orifices, arranged in the form of a pyramid or cone, facing upwind. The individual pressures reflect the effects of local flow direction and dynamic and total pressure. Figure 1 shows a schematic diagram and photograph of a typical probe constructed from standard stainless steel tubing. The tube faces have been ground to an included angle of 90 degrees, in the form of a pyramid in which the peripheral orifices are aligned to planes 90 degrees apart. The central orifice, which measures total pressure, is ground normal to the probe axis.

2.0 METHOD OF PROBE CALIBRATION

2.1 Angles and Velocity Relative to the Probe

Since this probe is to be used in the non-nulling mode, the flow impinging on it will, in general, not be axial. It is therefore necessary to define angular and component velocity conventions which can be adapted both for calibration and use of the probe. Figure 2 illustrates these angles and velocities in the vector diagram, as follows:

AO is the resultant flow velocity vector impinging on the probe, whose axis is aligned along OC. The flow direction in the upwash, or α-plane is the angle BOC; flow direction in the sidewash or β-plane is the angle DOC. The velocity components associated with the resultant velocity V_R are (in aircraft terminology) longitudinal component u (vector CO), upwash w (vector BC) and side-wash v (vector DC).

The angles θ and ϕ are the pitch angle COA of the resultant velocity vector in the α-β plane COA, and the roll angle BCA in the cross flow plane ABCD respectively.

2.2 Orifice Pressure Coefficients

Before defining orifice pressure coefficients, it is necessary to specify a numbering system, and this is illustrated in the sketch as shown below.

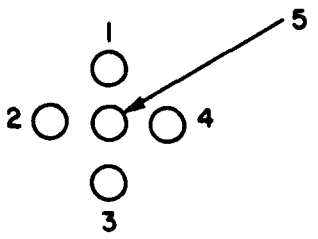

SKETCH (i) – PROBE ORIFICE ORIENTATION LOOKING DOWNSTREAM

Looking downstream, the peripheral holes are numbered one to four in a counter clockwise direction. Holes one and three are sensitive to flow angularity in the pitch plane while holes two and four are sensitive to flow angularity in the yaw plane. The central or fifth hole measures total pressure, as modified by the inclination of the resultant flow vector.

As in normal wind tunnel procedure, all pressures are measured relative to a reference static pressure, p_o, such as the working section static pressure. The pressure coefficients corresponding to each of the probe orifices are:

$$C_{p1} = \frac{p_1 - p_o}{p_T - p_o} \tag{1}$$

$$C_{p2} = \frac{p_2 - p_o}{p_T - p_o} \tag{2}$$

$$C_{p3} = \frac{p_3 - p_o}{p_T - p_o} \tag{3}$$

$$C_{p4} = \frac{p_4 - p_o}{p_T - p_o} \tag{4}$$

$$C_{p5} = \frac{p_5 - p_o}{p_T - p_o} \tag{5}$$

$$\bar{C}_p = \frac{1}{4}(C_{p1} + C_{p2} + C_{p3} + C_{p4}) \tag{6}$$

p_T is the tunnel reference total pressure, measured upstream of the probe, (usually in the tunnel settling chamber) and $\bar{C}_p$ is the average of all the peripheral pressure coefficients. Thus $p_T - p_o$ is effectively the tunnel (or ambient flow) dynamic pressure, and is *not* measured by the five-hole probe but from the two auxiliary pressure taps. Listings of the pressure coefficients C_{p1} to C_{p5} obtained in a calibration of a five-hole probe, are presented in Appendix B.

2.3 Probe Calibration Parameters

In order to describe the probe calibration procedure, it is necessary to define dimensionless parameters as follows:

Pitch Plane Parameter R (upwash)

$$R = \frac{C_{p3} - C_{p1}}{C_{p5} - \bar{C}_p} \tag{7}$$

Yaw Plane Parameter Q (sidewash)

$$Q = \frac{C_{p2} - C_{p4}}{C_{p5} - \bar{C}_p} \tag{8}$$

The sign convention for Q, R, α, β, and v, w is based on normal wind-tunnel conventions, as indicated in Figure 2.

Dynamic and static pressure parameters P and S are defined as follows:

$$P = C_{p5} - \bar{C}_p \tag{9}$$

$$S = \frac{1 - C_{p5}}{C_{p5} - \bar{C}_p} \tag{10}$$

In a smooth uniform flow directed along the probe axis, $\bar{C}_p$ is equivalent to the static pressure measured at the side holes on a pitot-static tube, and C_{p5} to the total pressure measured at the probe tip. Thus P is seen to be equivalent to the flow dynamic pressure for smooth uniform flow; in general, however, P is a measure of the local "dynamic" pressure when the real flow is both disturbed and oblique.

Since C_{p5} is a measure of local total pressure, then $1 - C_{p5}$ is a measure of local static pressure, and has a value of zero when the probe is fully aligned with the flow. The parameter S therefore, is a measure of local static pressure expressed as a fraction of the local dynamic pressure.

It is important to emphasize that the probe reference pressures p_o and p_T must be measured at the same corresponding tunnel wall taps during calibration as in flow measurement; usually p_o is the working section sidewall static pressure, and p_T the settling chamber total pressure.

2.4 Pitch and Yaw Angles of the Flow

The pitch and yaw angles to which the probe is set during calibration are defined as α, in the upwash plane, and β in the sidewash plane. Other angles, θ and ϕ, which are useful in interpreting calibration data are illustrated in Figure 2, and are defined as follows:

θ is the angle between the resultant vector and the probe axis, in the combined α-β plane COA.

ϕ is the roll angle BCA of the component resultant velocity vector in a plane normal to the probe axis.

A relationship between these angles is as follows:

$$\theta = \text{Arcsin}\left[\sqrt{\text{Sin}^2\beta + \text{Cos}^2\beta \cdot \text{Sin}^2\alpha}\right] \tag{11}$$

$$\phi = \text{Arctan}\left[\frac{\text{Tan}\,\beta}{\text{Tan}\,\alpha}\right] \tag{12}$$

and the inverse relations are: α = Arctan (Tan θ · Cos ϕ), β = Arctan (Tan θ · Sin ϕ). The angle θ is always positive in the range $0 < \theta < 90°$. The angle ϕ is always positive in the range $0 < \phi < 360°$. The angles α and β are in the range $-90° < \alpha, \beta < +90°$. The five-hole probe cannot normally be used to measure flow angles outside of a cone angle θ of 45°. For larger flow angles, a modified calibration procedure can be used, or a seven-hole probe.

3.0 PROBE CALIBRATION CHARACTERISTICS

In calibrating the probe, the maximum values to which the pitch and yaw angles α and β were set were ± 45°. The response of each set of side hole pressure differentials was linear up to about 30 degrees when pitched in its own plane; they were insensitive to small departures of inclination in the opposite plane. A typical value for the side-hole sensitivity is

$$K = \frac{\Delta P}{1/2\,\rho\,V_T{}^2\Delta\alpha} = 0.0583 \text{ per degree}$$

Figures (i) - (x) of Appendix A show the response of each individual probe orifice in terms of either the resultant angle θ in the combined pitch plane, or the roll angle ϕ in the probe crosswind plane. The central orifice C_{p5} is seen to be affected mainly by pitch and only very slightly by roll angle ϕ; its pressure varies from full total pressure in unskewed flow, to about 70% of this when the resultant velocity inclination is 30 degrees. As the inclination of the resultant velocity increases, the pressure sensed by the central hole drops more rapidly.

The pressure in any of the peripheral holes changes significantly with both θ and ϕ. When ϕ = 0° or 90° or 180° or 270°, i.e., the resultant flow in either of the pitch or yaw planes, the pressure on the windward orifice gradually increases until total pressure is achieved near θ = 45°.

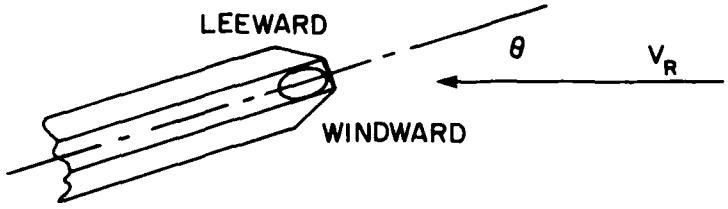

At the same time, the pressure on the leeward orifice decreases rapidly as suction is established on the probe head due possibly to a flow detachment on that side.

If the probe is also inclined in the opposite plane, ($0 < \phi < 90°$) the characteristic of the windward orifice changes considerably, but that of the leeward orifice, not so much.

The calibration-parameters P, Q, R and S have been found to be fairly simple functions of the resultant pitch angle θ and the roll angle ϕ. Since the parameter Q is sensitive to the yaw component, and R to the pitch component, then Q/R should be zero for a flow with no yaw component, and large for a flow with no pitch component. Hence Arctan (Q/R) is a measure of the roll angle ϕ in the plane normal to the probe axis. Similarly, $\sqrt{Q^2 + R^2}$ is a measure of the magnitude of the velocity vector, and should be approximately independent of roll angle ϕ, for a resultant flow vector that lies on a cone of constant semi-apex angle θ.

The angle ϕ is a scalar quantity, and is determined only in the lower left cross-plane quadrant as shown in Figure 2. The velocity components as determined from θ and ϕ are also scalar and their

signs and the signs of the angles in the α and β planes must then be assigned according to the signs of Q and R as originally determined by Equations 7 and 8. The actual cross-plane resultant vector (AC, Fig. 2) will in general, rotate around the longitudinal axis, as the oncoming flow may take up any orientation; the actual relationships between the roll angle ϕ and the parameters Q and R are listed as follows:

if $Q > 0$, $R > 0$ then ϕ is as calculated from Equation (14), i.e. $\phi = \phi$ (14)

if $Q > 0$, $R < 0$ then $\phi = 180 - \phi$ (14)

if $Q < 0$, $R < 0$ then $\phi = 180 + \phi$ (14)

if $Q < 0$, $R > 0$ then $\phi = 360 - \phi$ (14)

These functions, i.e. Arctan|Q/R| and $\sqrt{Q^2 + R^2}$ are shown in Figures 3(a), 3(b) and 4, plotted against ϕ and θ respectively. The dynamic and static pressure parameters P_{CAL} and S_{CAL} are also functions of the two angles θ and ϕ and are illustrated in Figures 5 and 6.

3.1 Empirical Representation of the Calibration Data

Empirical expressions which satisfactorily represent the average of Figure 3 (shown as Fig. 3(a) and 4(a)) experimental data, for both θ and ϕ are as follows:

Pitch angle θ

$$\theta = A_1 \sqrt{Q^2 + R^2} + A_2 (Q^2 + R^2) + A_3 (Q^2 + R^2)^{3/2} + A_4 (Q^2 + R^2)^2 \qquad (13)$$

where

$$A_1 = 8.6603$$
$$A_2 = 0.9708$$
$$A_3 = -0.033444$$
$$A_4 = 0.019914$$

These constants are for a typical probe. The resulting angle θ is in degrees ($0 < \theta < 90°$).

Roll angle ϕ

$$\phi = B_1 \, \mathrm{Tan}^{-1} \left|\frac{Q}{R}\right| + B_2 \left(\mathrm{Tan} \left|\frac{Q}{R}\right|\right)^2 + B_3 \left(\mathrm{Tan}^{-1} \left|\frac{Q}{R}\right|\right)^3 + B_4 \left(\mathrm{Tan}^{-1} \left|\frac{Q}{R}\right|\right)^4 \qquad (14)$$

where $\mathrm{Tan}^{-1} \left|\frac{Q}{R}\right|$ is in radians, and

$$B_1 = 95.825$$
$$B_2 = -75.034$$
$$B_3 = 33.981$$
$$B_4 = -1.2199$$

The resulting angle ϕ is in degrees ($0 < \phi < 90°$). The signs of Q and R will determine which quadrant ϕ lies in, as in 3.0 above.

The dynamic and static pressure parameters P_{CAL} and S_{CAL} can also be represented empirically as functions of θ and ϕ, as follows:

Dynamic pressure parameter P_{CAL} (θ, ϕ) as determined from calibration

$$P_{CAL}(\theta, \phi) = C_0 + C_1\theta + C_2\theta^2 + C_3\theta^3 \tag{15}$$

where: $C_0 = 0.504$ for a typical probe

$$C_1 = D_1 + D_2\phi + D_3\phi^2 + D_4\phi^3 + D_5\phi^4 + D_6\phi^5$$

$$C_2 = E_1 + E_2\phi + E_3\phi^2 + ... + E_6\phi^5$$

$$C_3 = F_1 + F_2\phi + F_3\phi^2 + ... + F_6\phi^5$$

The angles θ and ϕ are in degrees; however the angle ϕ is limited to 45°. If $\phi > 45°$ as determined from Equation (14), then the complement of ϕ must be used (i.e. $90 - \phi$), in Equation (15).

The constants Di, Ei and Fi are presented in Table I for a typical probe.

Static pressure parameter S_{CAL} (θ, ϕ) as determined from calibration

$$S_{CAL}(\theta, \phi) = G_1\theta^2 + G_2\theta^4 + G_3\theta^6 + G_4\theta^8 + G_5\theta^{10} \tag{16}$$

where:

$$G_1 = J_1 + J_2\phi + J_3\phi^2 + J_4\phi^3 + J_5\phi^4$$

$$G_2 = K_1 + K_2\phi + K_3\phi^2 + K_4\phi^3 + K_5\phi^4$$

$$G_3 = L_1 + L_2\phi + L_3\phi^2 + L_4\phi^3 + L_5\phi^4$$

$$G_4 = M_1 + M_2\phi + M_3\phi^2 + M_4\phi^3 + M_5\phi^4$$

$$G_5 = N_1 + N_2\phi + N_3\phi^2 + N_4\phi^3 + N_5\phi^4$$

where θ and ϕ are in degrees. If ϕ is greater than 45° as determined from Equation (14), then the complement of ϕ is used (i.e. $90 - \phi$) in Equation (16).

The constants Ji, Ki, Li, Mi, Ni are presented in Table II for a typical probe.

4.0 USE OF THE PROBE IN AN UNKNOWN FLOW

In normal testing technique, the five orifices of the probe are connected to a differential transducer via sequential porting of a Scanivalve system. Tunnel reference pressure p_o is on the back of the transducer, and tunnel total pressure p_T is also scanned in sequence. If all five probe orifice pressures are required simultaneously, then five transducers and Scanivalve heads can be used, with tunnel p_o and p_T both connected to each separate unit.

Typical flow measuring techniques use either (a) a single five-hole probe connected to a single differential pressure transducer mounted in a single Scanivalve, (b) a single probe connected directly to five differential transducers and no Scanivalve is used, or (c) a rake of five-hole probes connected to five transducers mounted in five Scanivalve units. In all cases it is assumed that all the pressure transducers are referenced to tunnel static pressure p_o.

For setup (a), the five orifice pressures are sampled sequentially, so no flow computations can begin until all seven pressures are sampled. This has the disadvantage that in highly unsteady flows, the flow condition that existed when orifice pressure No. 1 was sampled may not be the same as when pressure No. 5 is sampled. The advantage of setup (a) is that only a single transducer, Scanivalve, and ADC (analog-to-digital converter) channel are required.

The usual plumbing hookup is with tunnel static pressure p_o on the first Scanivalve port, p_T on the second port and a calibration pressure if required on the third. Probe pressures No. 1 to No. 5 are on the next five ports, followed by the reference total and static pressures again on the ninth and tenth ports respectively. This type of hookup allows for the transducer tare to be measured (even with wind on) as the first and last measurement, so that transducer drift corrections can be applied to the intermediate measurements, if required.

The advantage of setup (b) is that all seven pressures can be measured simultaneously, if seven ADC channels are used and the windspeed is measured at the same instant. Whereas in (b) all seven transducers must be calibrated by a separate operation before any measurements can begin, setup (a) provides an "on-line" calibration each time the third Scanivalve port is sampled. In setup (b) tares can be measured only when the wind is off. Calibration of the five transducers in this case can be performed by sliding a piece of Tygon tubing tightly over the head of the probe thus applying a known pressure simultaneously to all five channels.

For setup (c) using a rake of N five-hole probes, each of the Scanivalves has tunnel static pressure p_o on the first and last ports, tunnel total pressure on the second and next-to-last ports, and the known calibration pressure on the third port. Scanivalve No. 1 is connected to orifice No. 1 of all N probes. Scanivalves No. 2, 3, 4 and 5 are therefore connected to orifices No. 2, 3, 4 and 5 respectively of all N probes. Five ADC channels are used, and a total of (3 + N + 2) Scanivalve ports are required for N probes. This setup has the advantages of (i) on-line wind-on calibration and tares, (ii) the flow computations for a single probe can proceed immediately the Scanivalve has stepped past its port, and (iii) drift corrections can be applied at the end of the stepping sequence. As in setup (a) however, windspeed is measured only at the beginning and end of the sequence. Also, if the five Scanivalves become unsynchronized, the data gathered is meaningless. This latter problem can be eliminated with the use of ganged, multi-head Scanivalves driven off a single stepper unit, or of the "wafer switch" type of Scanivalve.

A modification of setup (c) using seven transducers and five Scanivalves provides for simultaneous measurement of windspeed and the five probe pressures. The p_o and p_T transducers must be calibrated separately however, and seven ADC channels are required.

With the seven quantities (p_o, p_T, p1, p2, p3, p4 and p5) available from the pressure-measuring system, the probe calibration routines developed in Section 3.0 will furnish the characteristics of the unknown flow in steps (a) to (g) as follows:

a) Compute probe orifice coefficients C_{p1}, C_{p2}, C_{p3}, C_{p4}, C_{p5} and $\bar{C}_p$ from Equations (1) to (6).

b) Compute the probe dimensionless parameters P, Q, R from Equations (9), (8) and (7), respectively:

$$P = C_{p5} - \bar{C}_p$$

$$Q = \frac{C_{p2} - C_{p4}}{P}$$

$$R = \frac{C_{p3} - C_{p1}}{P}$$

At this point, the signs of the parameters Q and R should be saved in the program for future use.

c) Compute the pitch and roll angles, θ and ϕ from the empirical Expressions (13) and (14), as follows:

$$\theta = A_1 \sqrt{Q^2 + R^2} + A_2 (Q^2 + R^2) + A_3 (Q^2 + R^2)^{3/2} + A_4 (Q^2 + R^2)^2$$

$$\phi = B_1 \, \text{Tan}^{-1} \left| \frac{Q}{R} \right| + B_2 \left(\text{Tan}^{-1} \left| \frac{Q}{R} \right| \right)^2 + B_3 \left(\text{Tan}^{-1} \left| \frac{Q}{R} \right| \right)^3 + B_4 \left(\text{Tan}^{-1} \left| \frac{Q}{R} \right| \right)^4.$$

The signs of Q and R will determine the correct quandrant for ϕ as in 3.0 above.

d) Compute the values of the angles α and β, and assign their signs according to the signs of Q and R, as follows:

$$\alpha = \text{Tan}^{-1} \left[\text{Tan}\, \theta \cdot \text{Cos}\, \phi \right] \tag{17}$$

$$\beta = \text{Tan}^{-1} \left[\text{Tan}\, \theta \cdot \text{Sin}\, \phi \right] \tag{18}$$

all angles are in degrees, $-90° < \alpha, \beta < +90°$.

e) Compute flow dynamic pressure and resultant velocity ratios using (Eq. (9) and (15)), as follows:

Local dynamic pressure

$$q/q_T = \frac{P}{P_{CAL}\,(\theta, \phi)} \tag{19}$$

where $P_{CAL}\,(\theta, \phi)$ is given by Equation (15) and P by Equation (9).

Local resultant velocity

$$\frac{V_R}{V_T} = \sqrt{q/q_T} \tag{20}$$

f) Compute the three velocity components $\frac{u}{V_T}$, $\frac{v}{V_T}$, $\frac{w}{V_T}$ from Equations (20), (13) and (14) (see Fig. 2), as follows:

Longitudinal velocity component

$$\frac{u}{V_T} = \left(\frac{V_R}{V_T}\right) \text{Cos}\,\theta \tag{21}$$

Yaw plane velocity component

$$\frac{v}{V_T} = \left(\frac{V_R}{V_T}\right) \text{Sin}\,\theta \cdot \text{Sin}\,\phi \tag{22}$$

Pitch plane velocity component

$$\frac{w}{V_T} = \left(\frac{V_R}{V_T}\right) \text{Sin}\,\theta \cdot \text{Cos}\,\phi \tag{23}$$

The signs of the components $\frac{v}{V_T}$ and $\frac{w}{V_T}$ are assigned according to the original signs of Q and R respectively, as determined in step (b).

g) **Compute local total pressure coefficient in the unknown flow**

The flow total pressure is sensed mainly by the central orifice of the probe, however the magnitude of C_{p5} must be corrected for the effects of flow inclination. The local total pressure coefficient C_{pt} is then computed as follows:

$$C_{pt} = \frac{p_t - p_o}{1/2\,\rho\,V_T^{\,2}} = C_{p5} + S_{CAL}\,(\theta, \phi) \cdot P \tag{24}$$

where $S_{CAL}\,(\theta, \phi)$ is given by Equation (16) and P by Equation (9). The local static pressure coefficient C_{ps} can be computed as follows:

$$C_{ps} = C_{pt} - q/q_T$$

5.0 CONCLUSIONS

This note has presented a method of calibration and use for five-hole flow direction probes. Since exploration of three-dimensional airflows frequently involves mixed regions of both propulsive and highly skewed flows, as well as dissipative wakes, this probe technique will furnish flow angles in two planes, three velocity components, and local total and static pressures.

The flow conditions under which this calibration was done corresponded to a low subsonic flow, at a unit Reynolds number of 10^6. The calibration constants given in Tables I and II, and other sections of this note refer to a specific probe which had been calibrated some time ago, and which is in routine use presently in the Laboratory. In general, all such probes, particularly those which may have head configurations different than that specified in Figure 1 should be individually calibrated. This note has not presented any details about the calibration installation and fixture but the probe should be positioned on the centreline of the wind tunnel, with degrees of freedom in upwash (α) and sidewash (β), or in pitch (θ) and roll (ϕ). A tunnel test section sidewall static pressure tap and a settling chamber total pressure probe should be used to obtain the references pressures p_o and p_T respectively.

6.0 BIBLIOGRAPHY

1. Bryer, D.W.
   Pankhurst, R.C.
   Pressure-Probe Methods for Determining Wind Speed and Flow Direction.
   HMSO, (NPL), 1971.

2. Wickens, R.H.
   South, P.
   Rangi, R.S.
   Henshaw, D.
   Experimental Developments in V/STOL Wind Tunnel Testing at the National Aeronautical Establishment.
   Can. Aeronautics and Space Inst., Vol. 19, No. 4, April 1973.

TABLE I

COEFFICIENTS FOR DYNAMIC PRESSURE FUNCTION $P_{CAL}(\theta, \phi)$ (Eq. (15))

i	Di	Ei	Fi
1	-49.6 x_e - 05	654 x_e - 07	-352 x_e - 08
2	15.8 x_e - 05	-124 x_e - 07	20.7 x_e - 08
3	-0.264 x_e - 05	3.54 x_e - 07	-0.678 x_e - 08
4	-7.24 x_e - 08	-2.48 x_e - 10	-8.4 x_e - 11
5	2.16 x_e - 09	-7.86 x_e - 11	3.71 x_e - 12
6	-1.33 x_e - 11	5.82 x_e - 13	-2.45 x_e - 14

Note: The values presented in Tables I and II represent those for a typical probe.

TABLE II

COEFFICIENTS FOR TOTAL PRESSURE FUNCTION S_{CAL} (θ, ϕ) (Eq. (16))

i	Ji	Ki	Li	Mi	Ni
1	9.288 x_e - 05	9.432 x_e - 07	-4.320 x_e - 10	7.398 x_e - 14	2.916 x_e - 17
2	1.561 x_e - 05	-5.927 x_e - 08	8.929 x_e - 11	-5.663 x_e - 14	1.485 x_e - 17
3	-1.611 x_e - 06	5.770 x_e - 09	-7.498 x_e - 12	4.882 x_e - 15	-1.498 x_e - 18
4	7.078 x_e - 08	-3.354 x_e - 10	5.585 x_e - 13	-4.227 x_e - 16	1.274 x_e - 19
5	-9.873 x_e - 10	5.349 x_e - 12	-9.743 x_e - 15	7.584 x_e - 18	-2.228 x_e - 21

Note: The values presented in Tables I and II represent those for a typical probe.

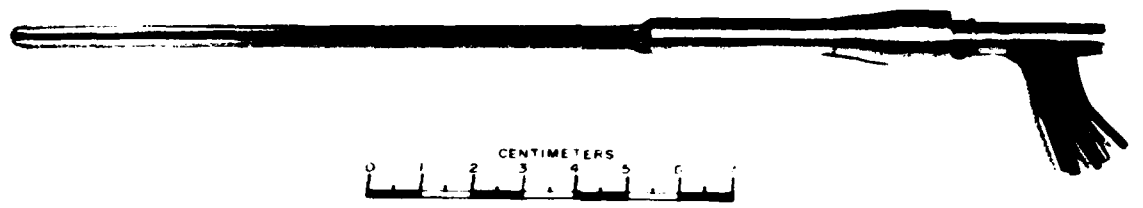

(a)

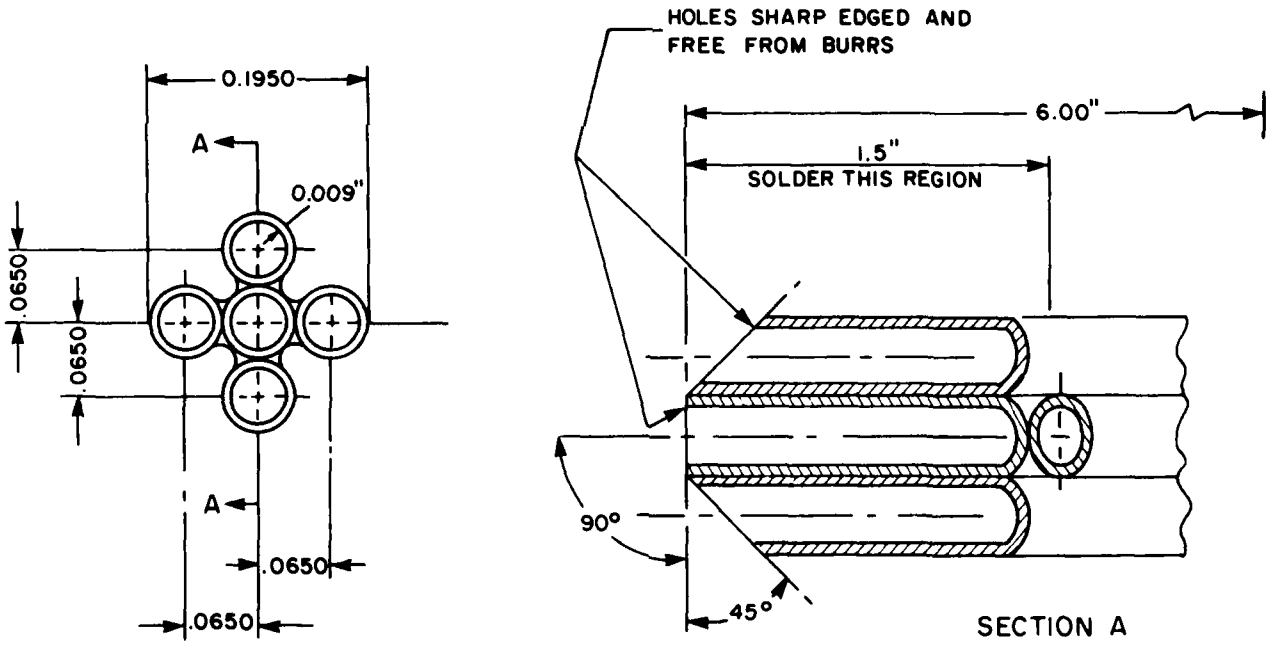

(b)

FIG. 1: GENERAL ARRANGEMENT AND DETAILS OF FIVE-HOLE FLOW DIRECTION PROBE

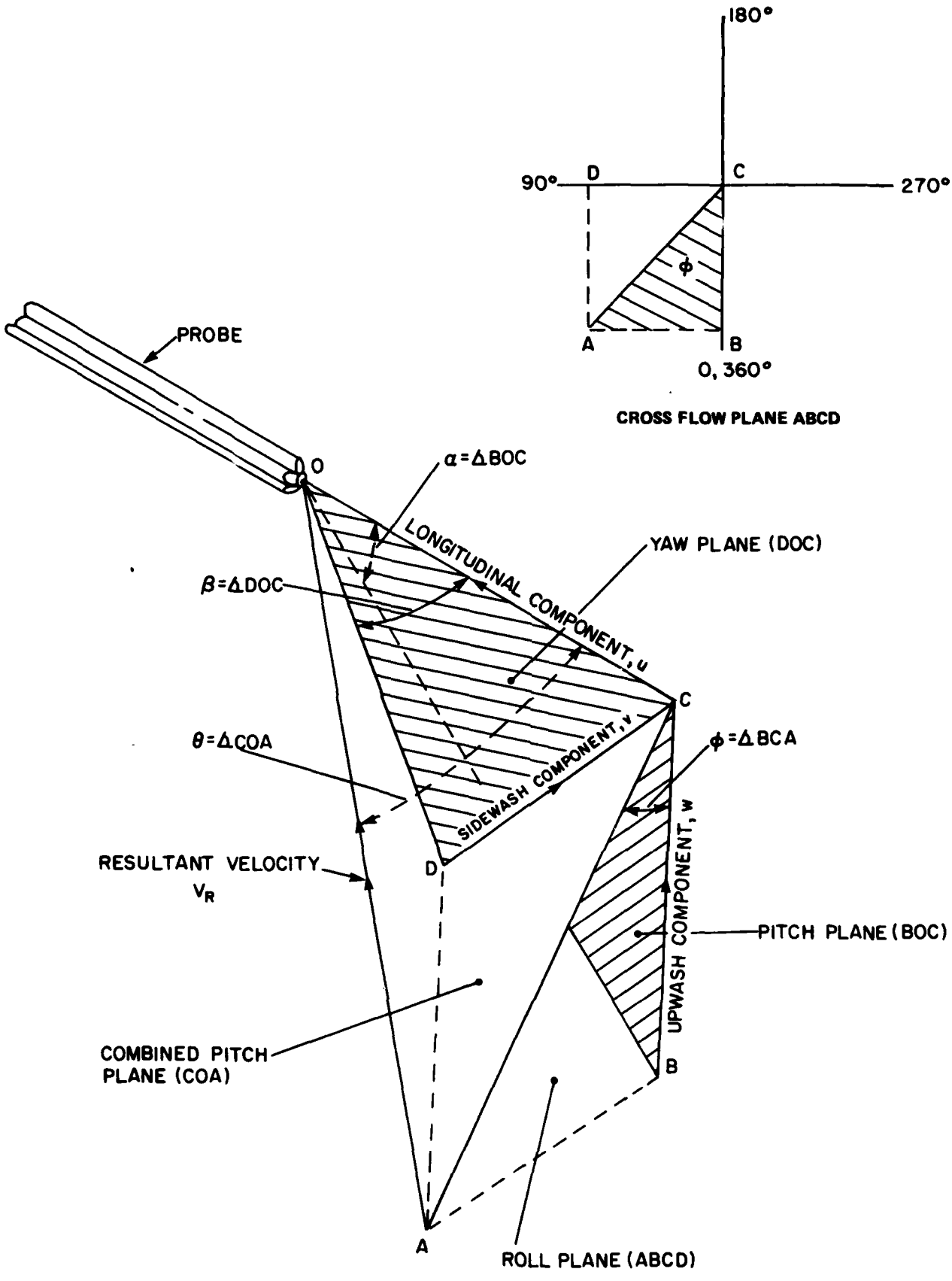

FIG. 2: ANGLE AND VELOCITY CONVENTIONS FOR A FIVE-HOLE FLOW DIRECTION PROBE

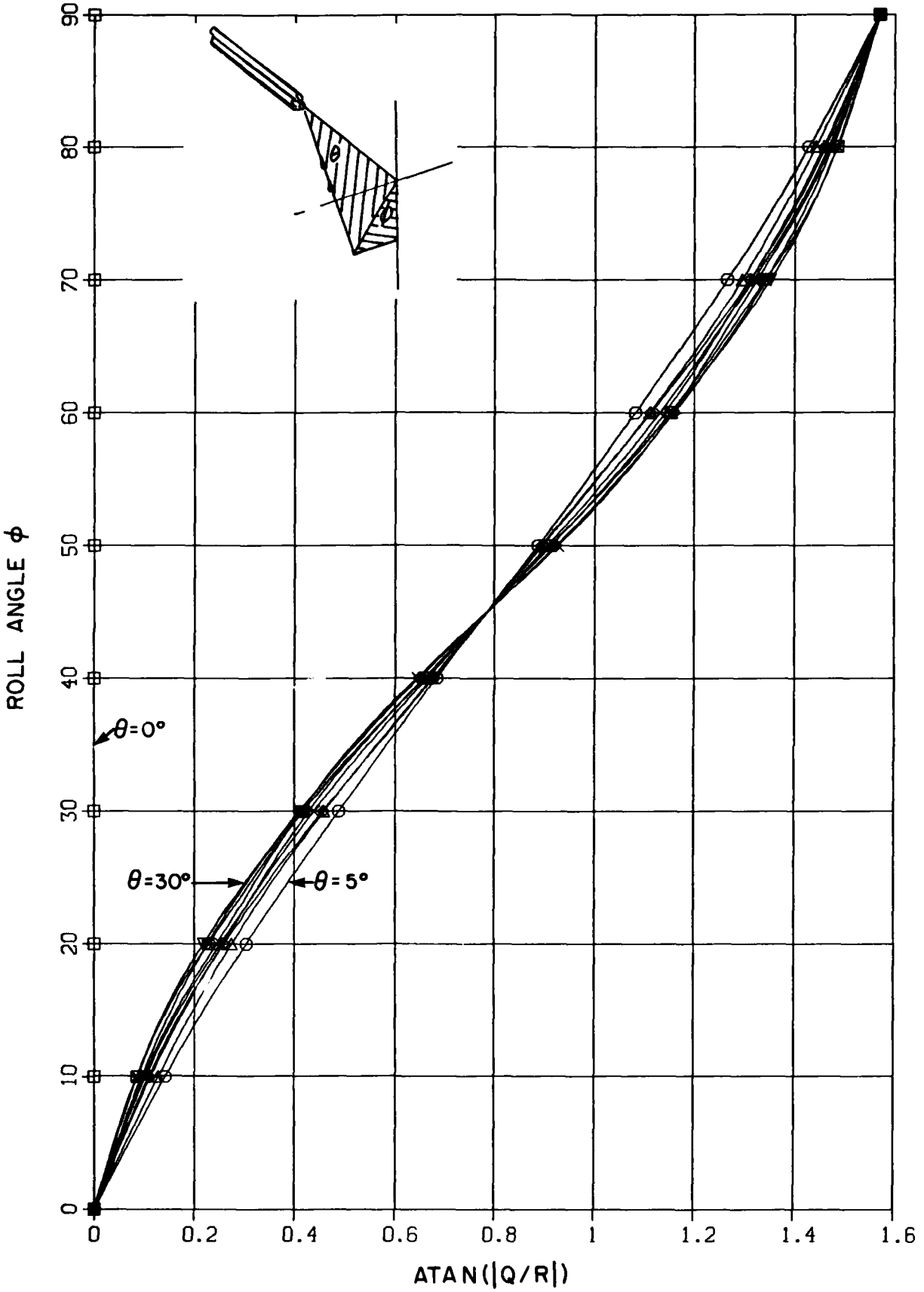

FIG. 3(a): PROBE ROLL ANGLE ϕ vs ARCTAN | Q/R |

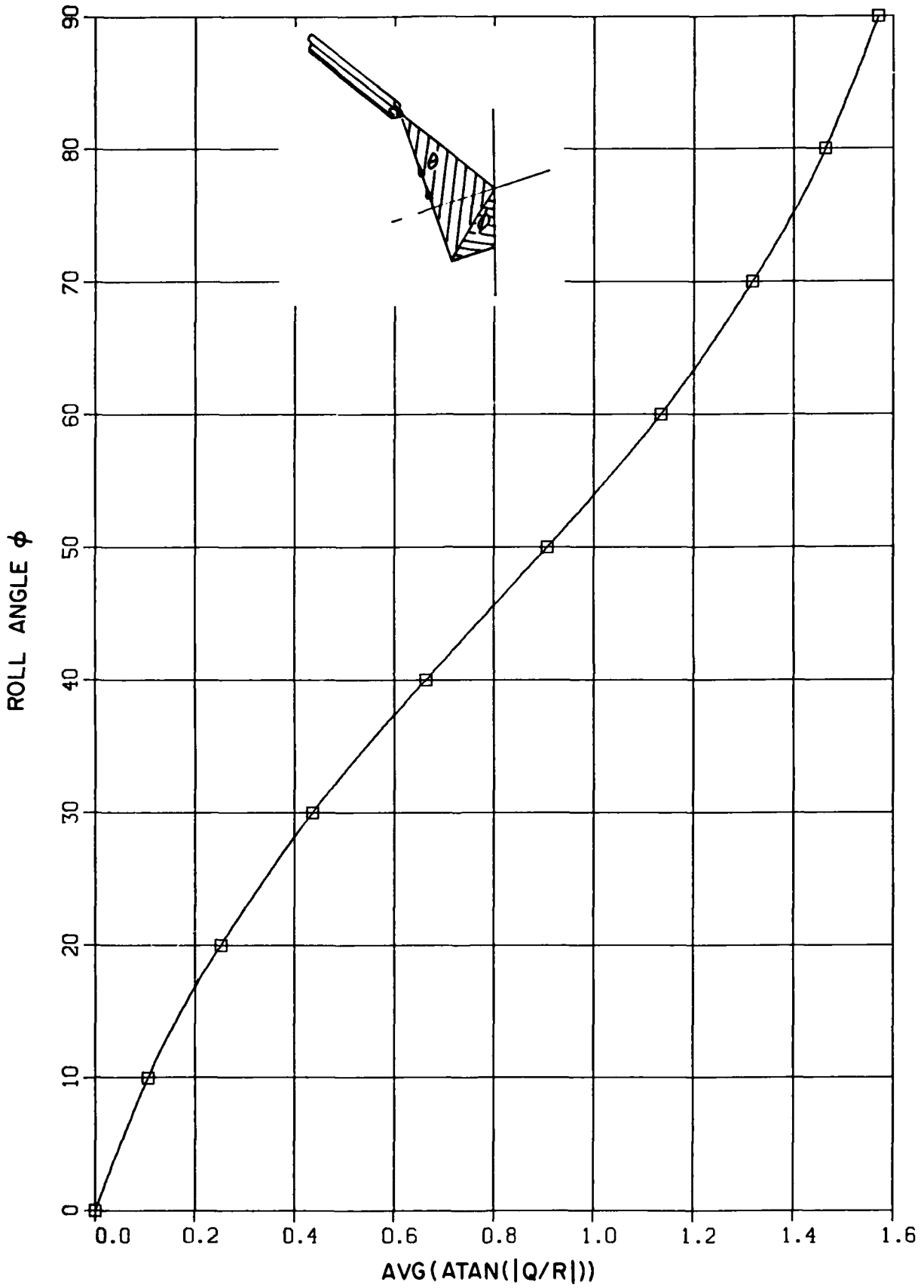

FIG. 3(b): PROBE AVERAGE ROLL ANGLE ϕ vs ARCTAN | Q/R |

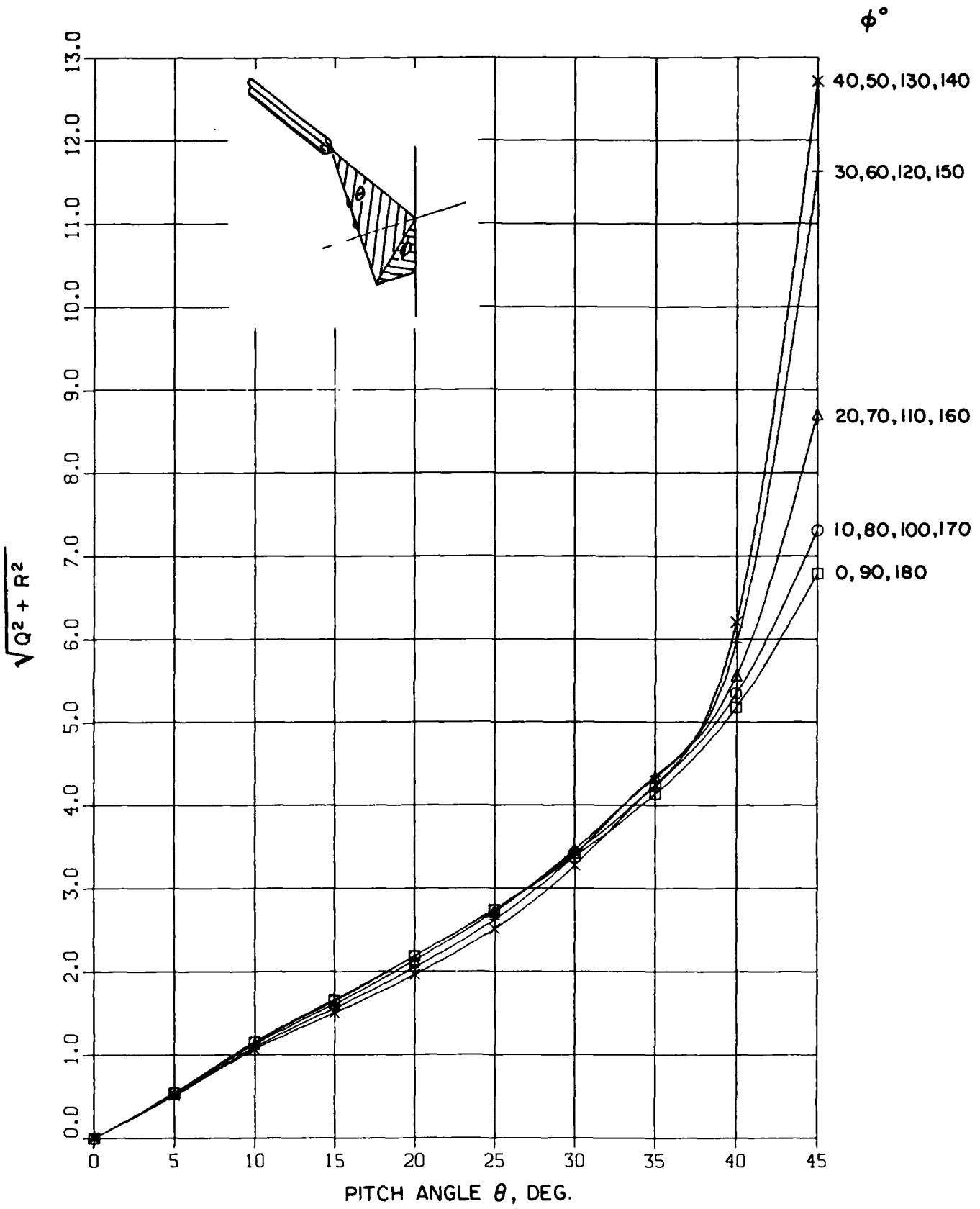

FIG. 4(a): PROBE PITCH ANGLE θ vs $\sqrt{Q^2 + R^2}$

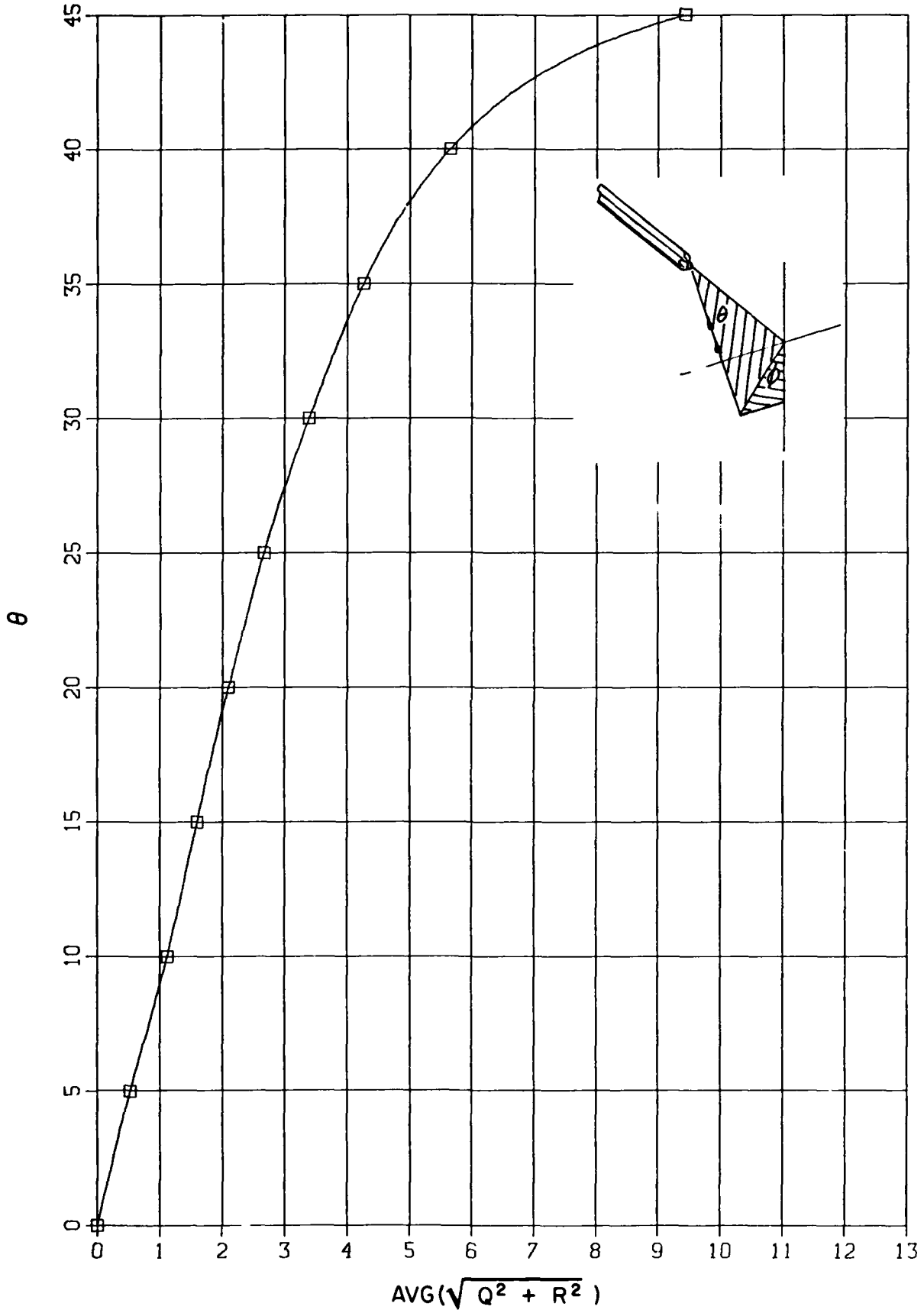

FIG. 4(b): PROBE AVERAGE PITCH ANGLE θ, DEGREES, vs $\sqrt{Q^2 + R^2}$

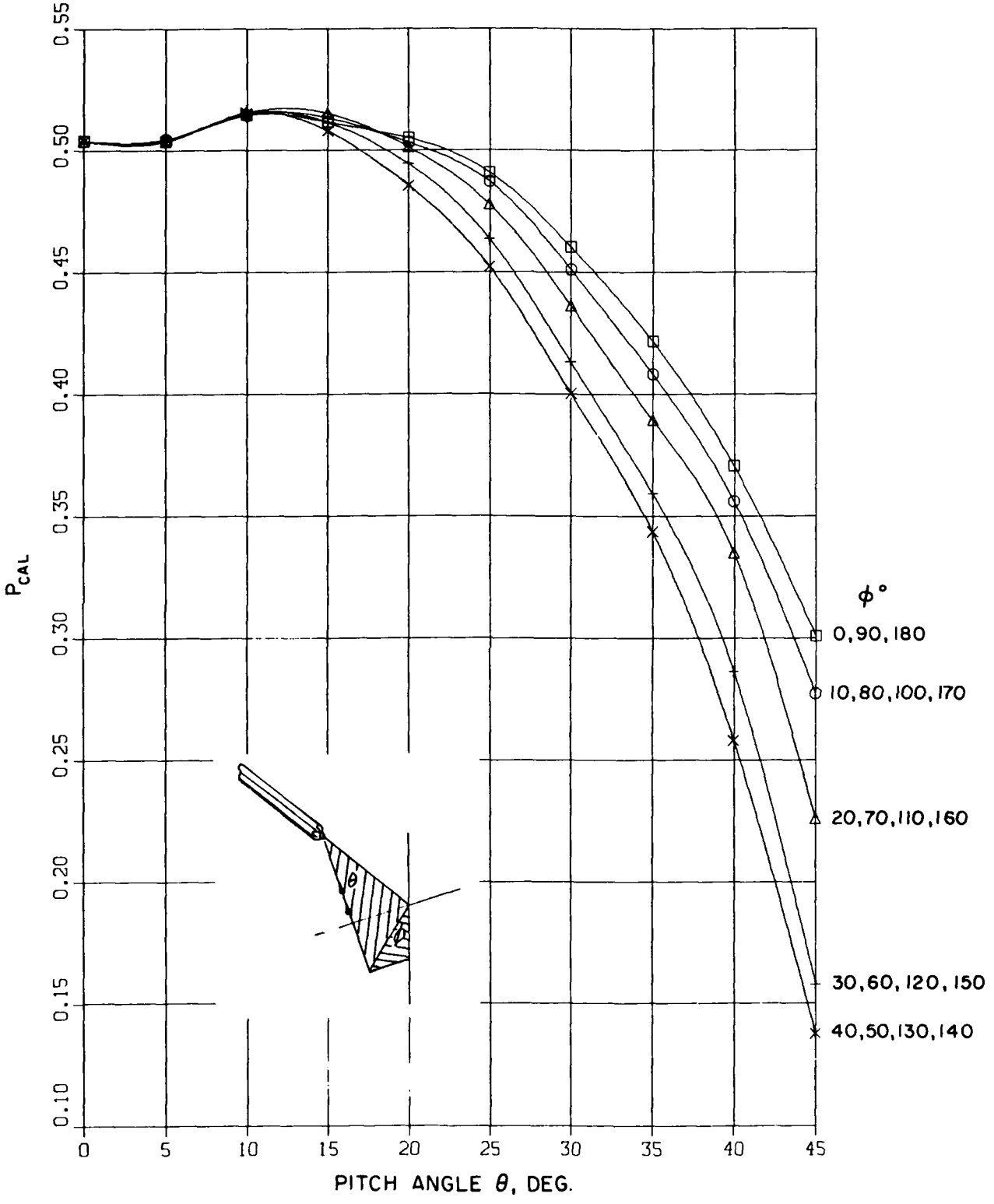

FIG. 5: PROBE DYNAMIC PRESSURE PARAMETER, $P = C_{p5} - \bar{C}_p$ vs PITCH ANGLE θ

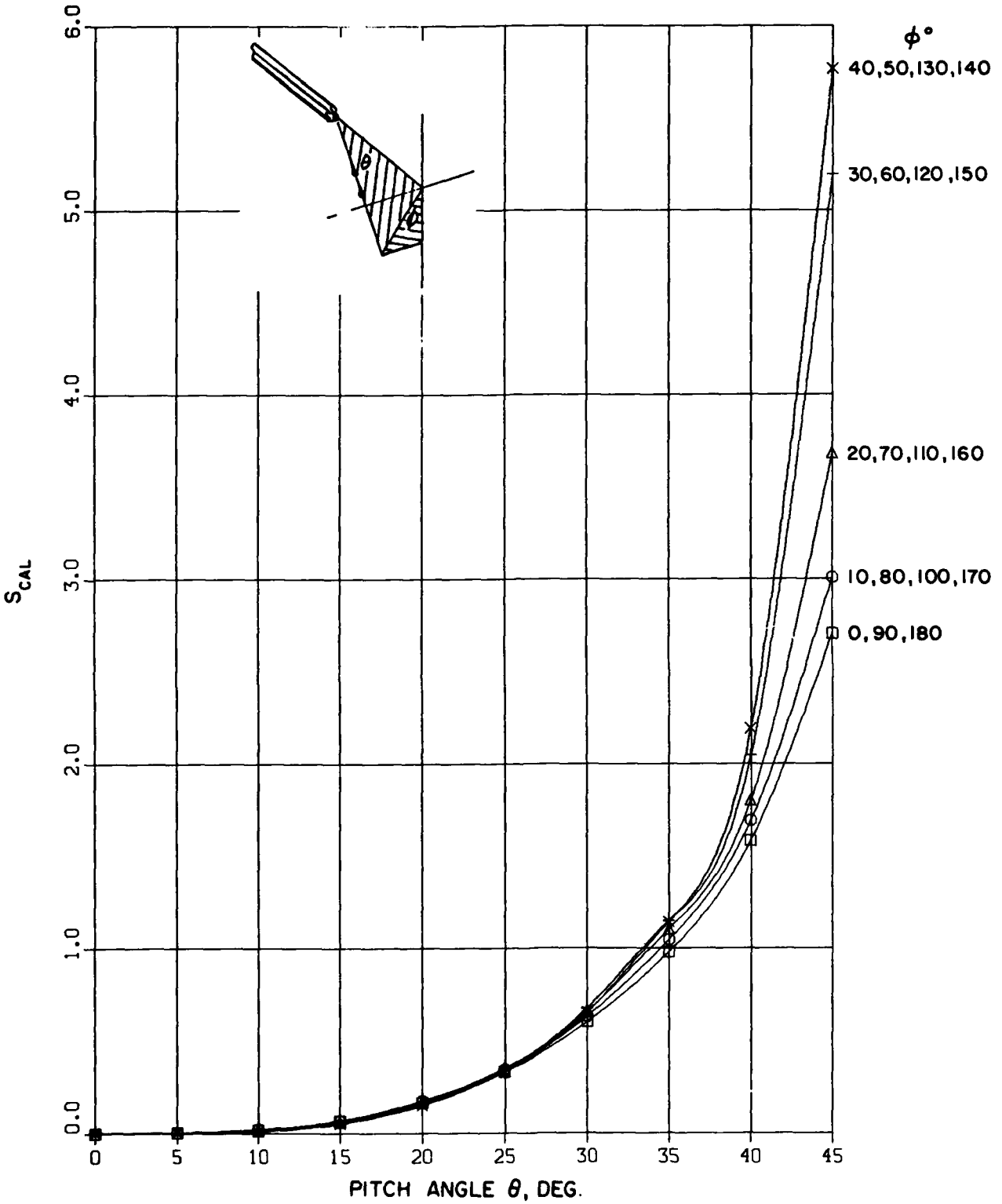

FIG. 6: PROBE STATIC PRESSURE PARAMETER, $S = \frac{1 - C_{p5}}{C_{p5} - \bar{C}_p}$ vs PITCH ANGLE θ

APPENDIX A

TYPICAL INDIVIDUAL PROBE ORIFICE PRESSURES COEFFICIENTS AS FUNCTIONS OF THE COMBINED PITCH ANGLE θ, AND ROLL ANGLE ϕ

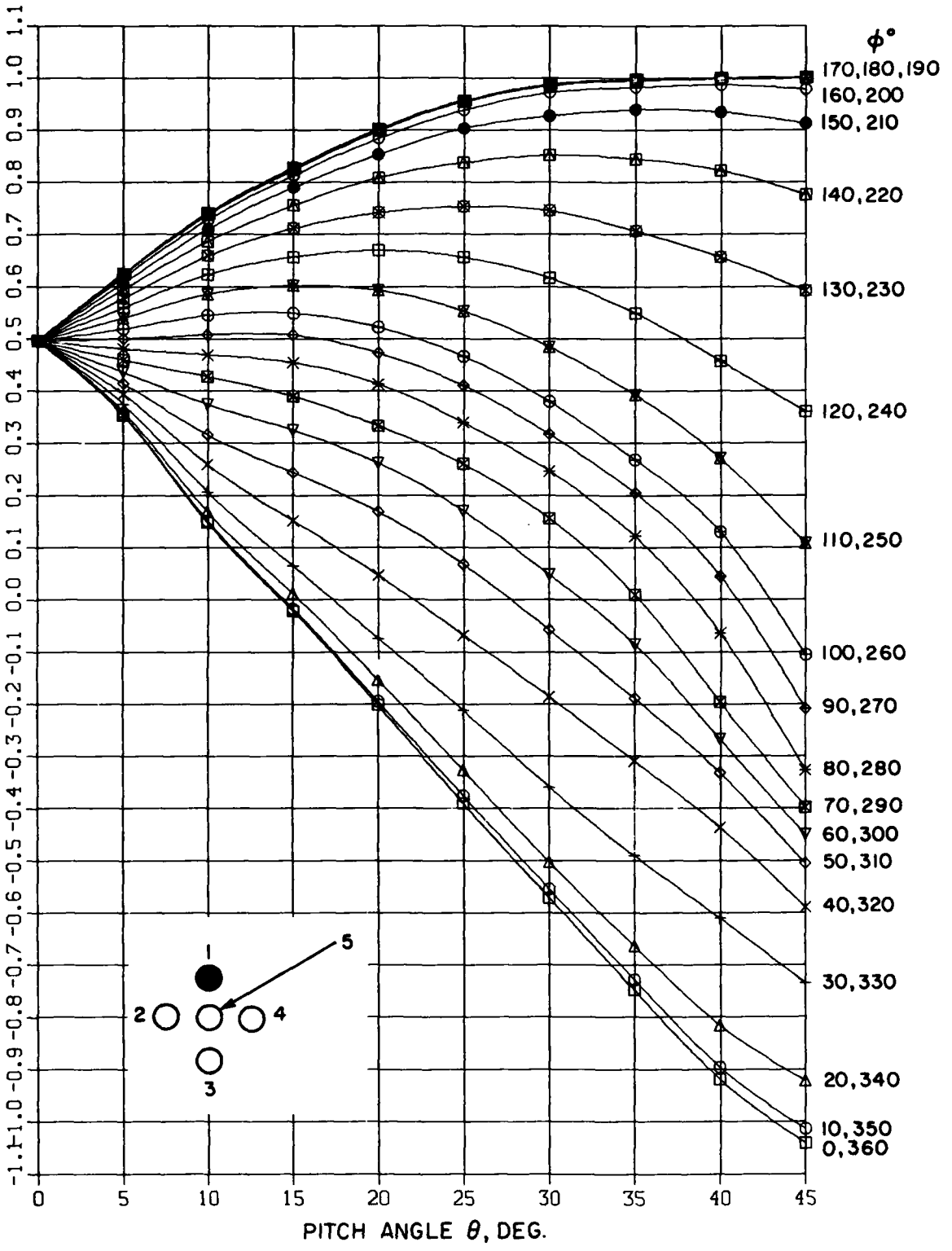

FIG. A1: PROBE SIDE ORIFICE PRESSURE COEFFICIENT, C_{p1}

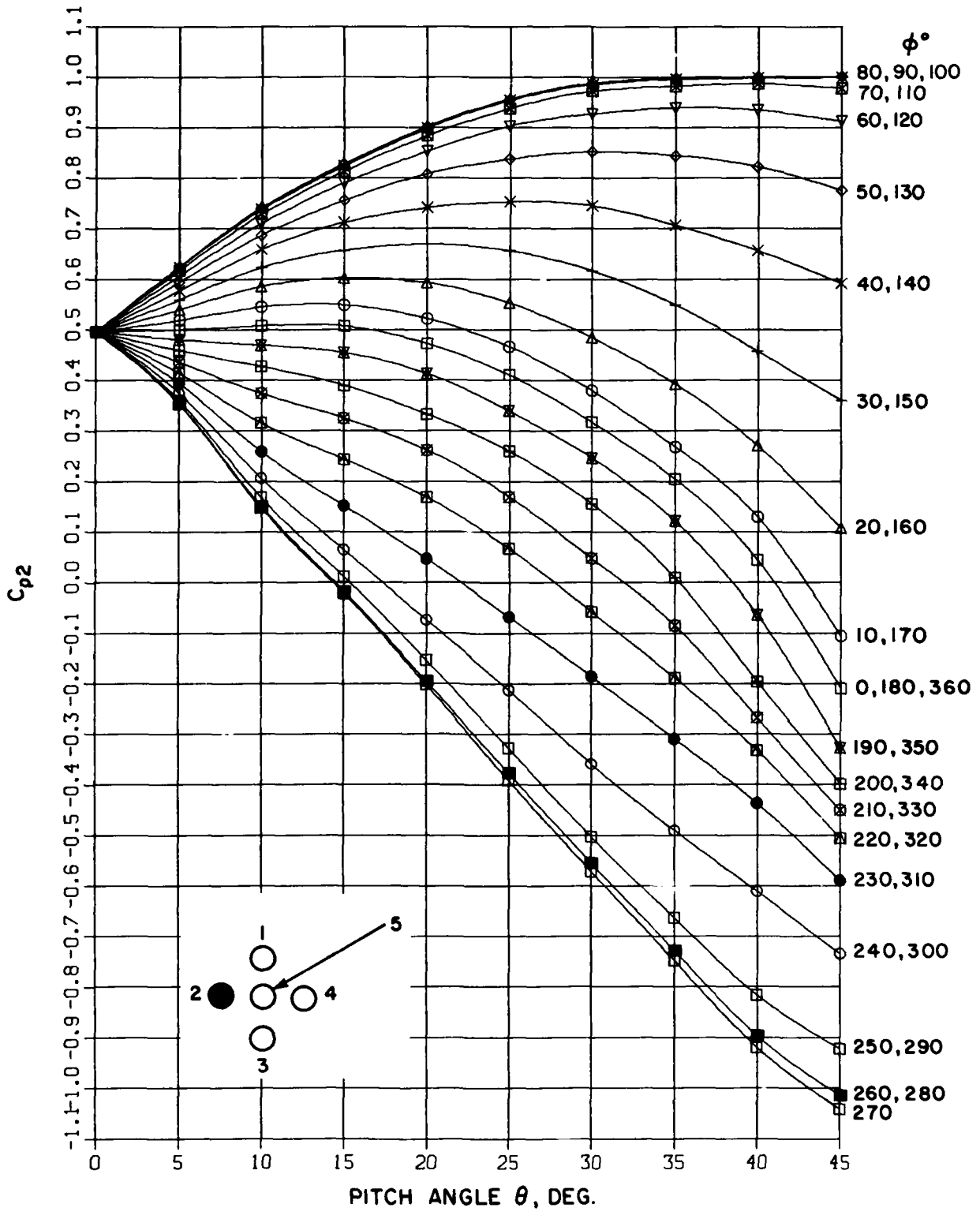

FIG. A2: PROBE SIDE ORIFICE PRESSURE COEFFICIENT, C_{p2}

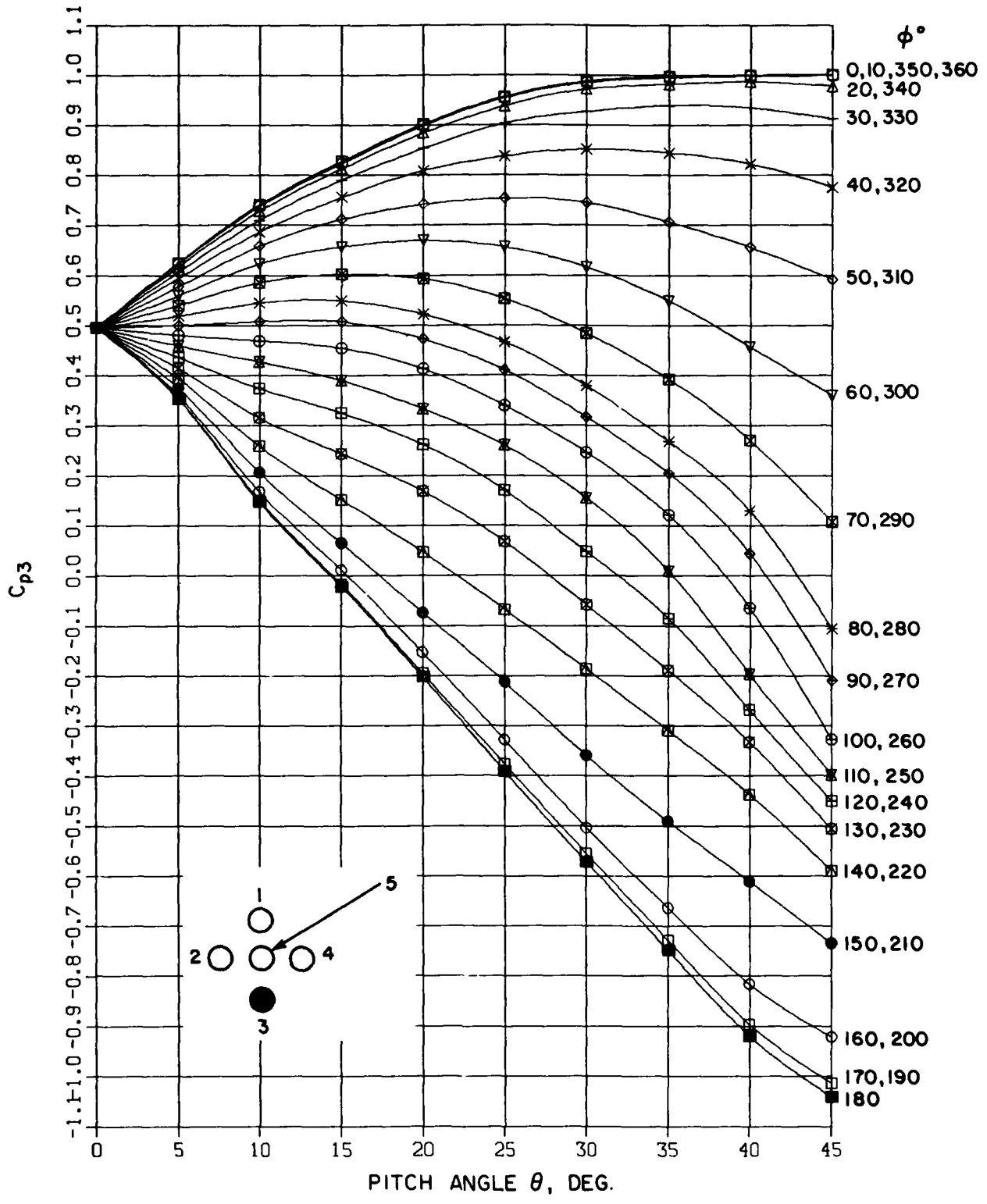

FIG. A3: PROBE SIDE ORIFICE PRESSURE COEFFICIENT, C_{p3}

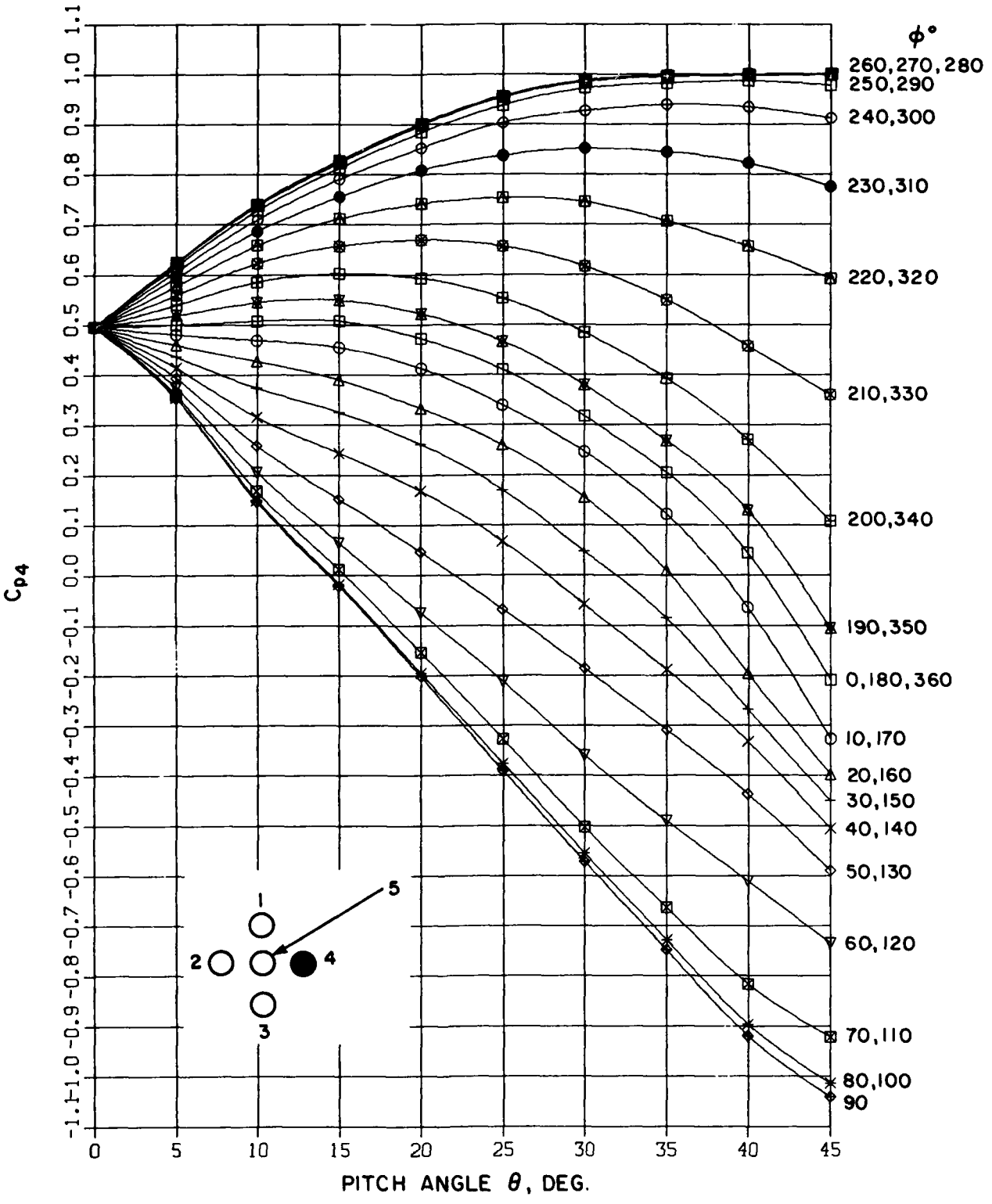

FIG. A4: PROBE SIDE ORIFICE PRESSURE COEFFICIENT, C_{p4}

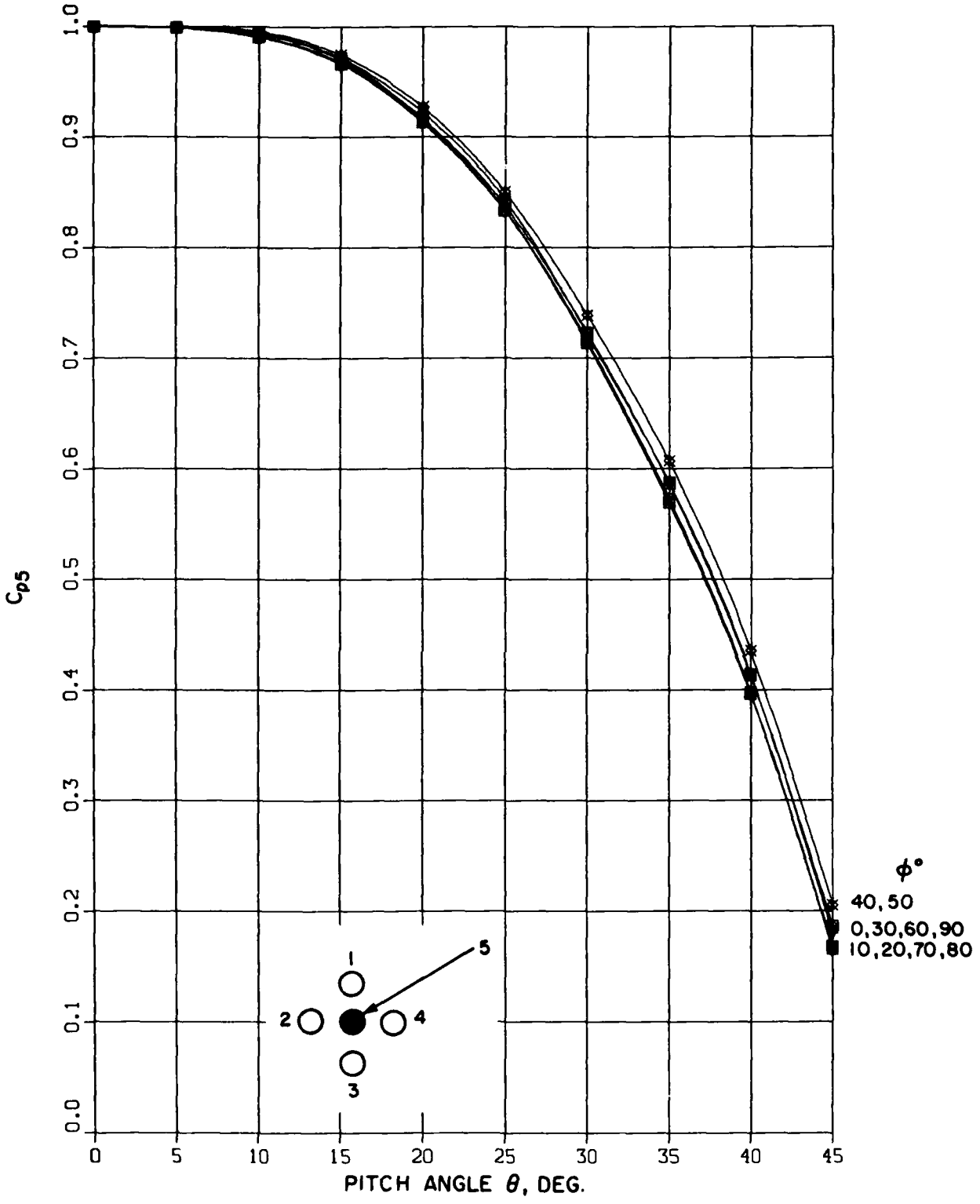

FIG. A5: PROBE CENTRAL ORIFICE PRESSURE COEFFICIENT, C_{p5}

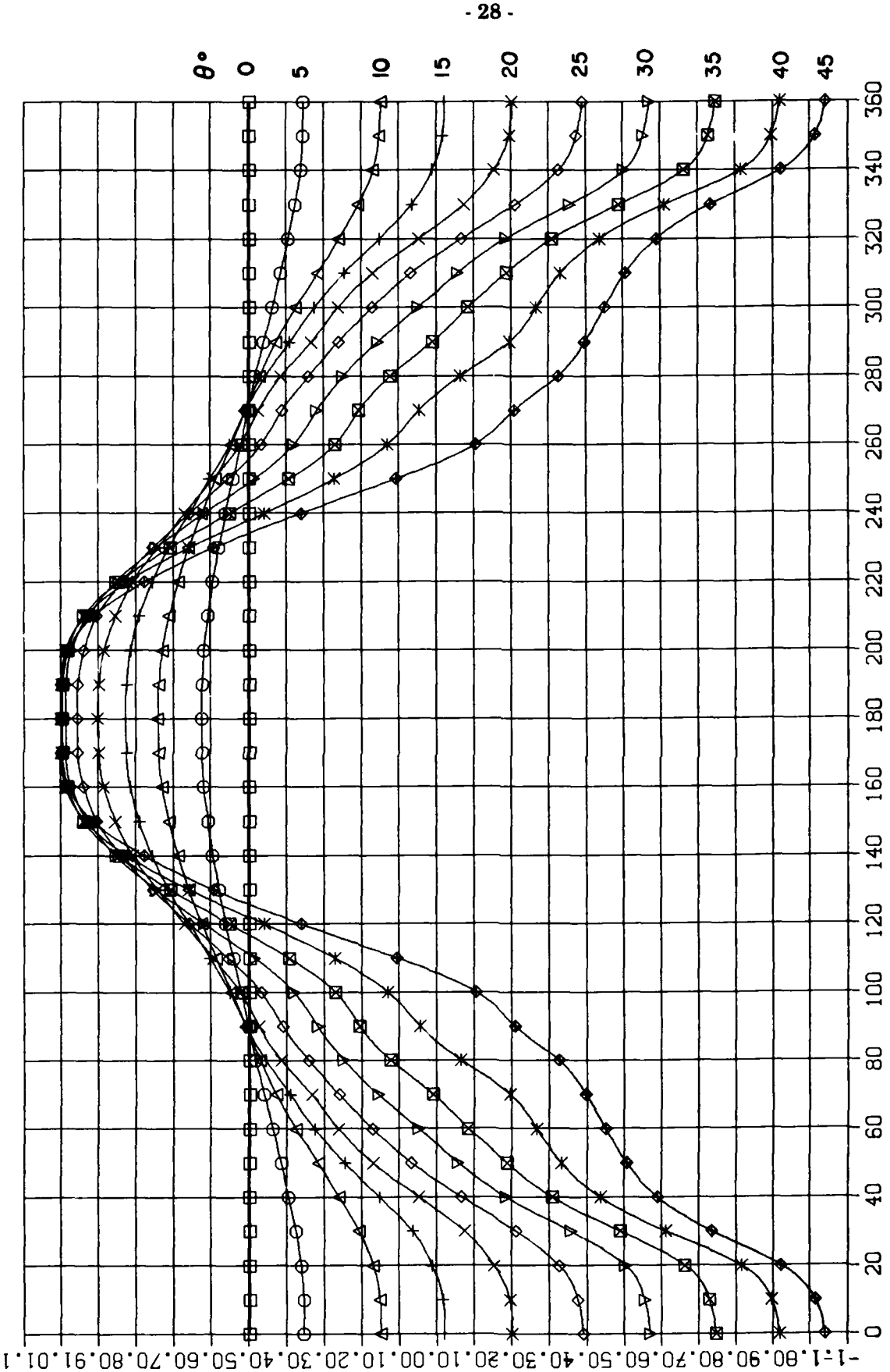

FIG. A6: PROBE SIDE ORIFICE PRESSURE COEFFICIENT, C_{pi}

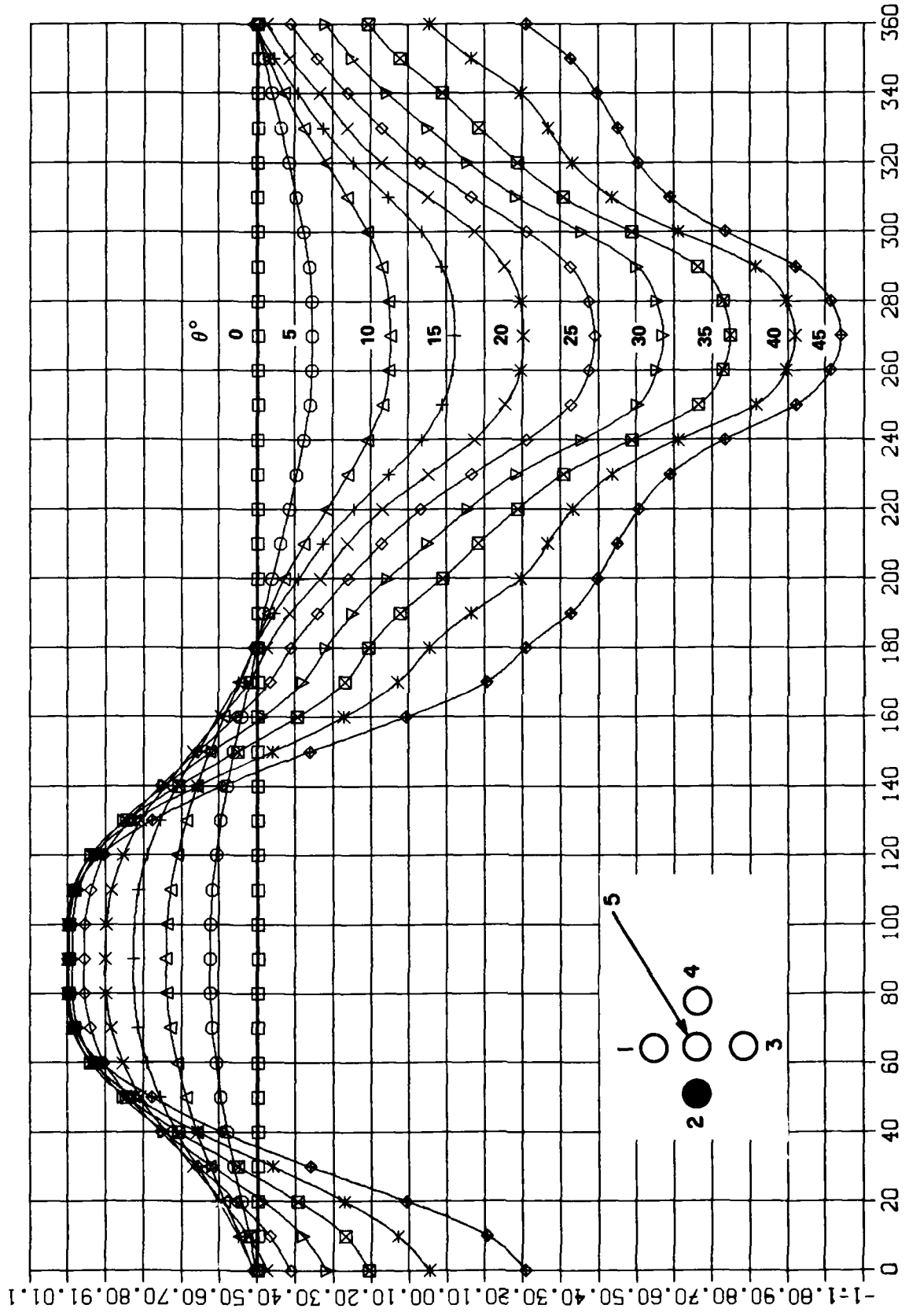

FIG. A7: PROBE SIDE ORIFICE PRESSURE COEFFICIENT, C_{p2}

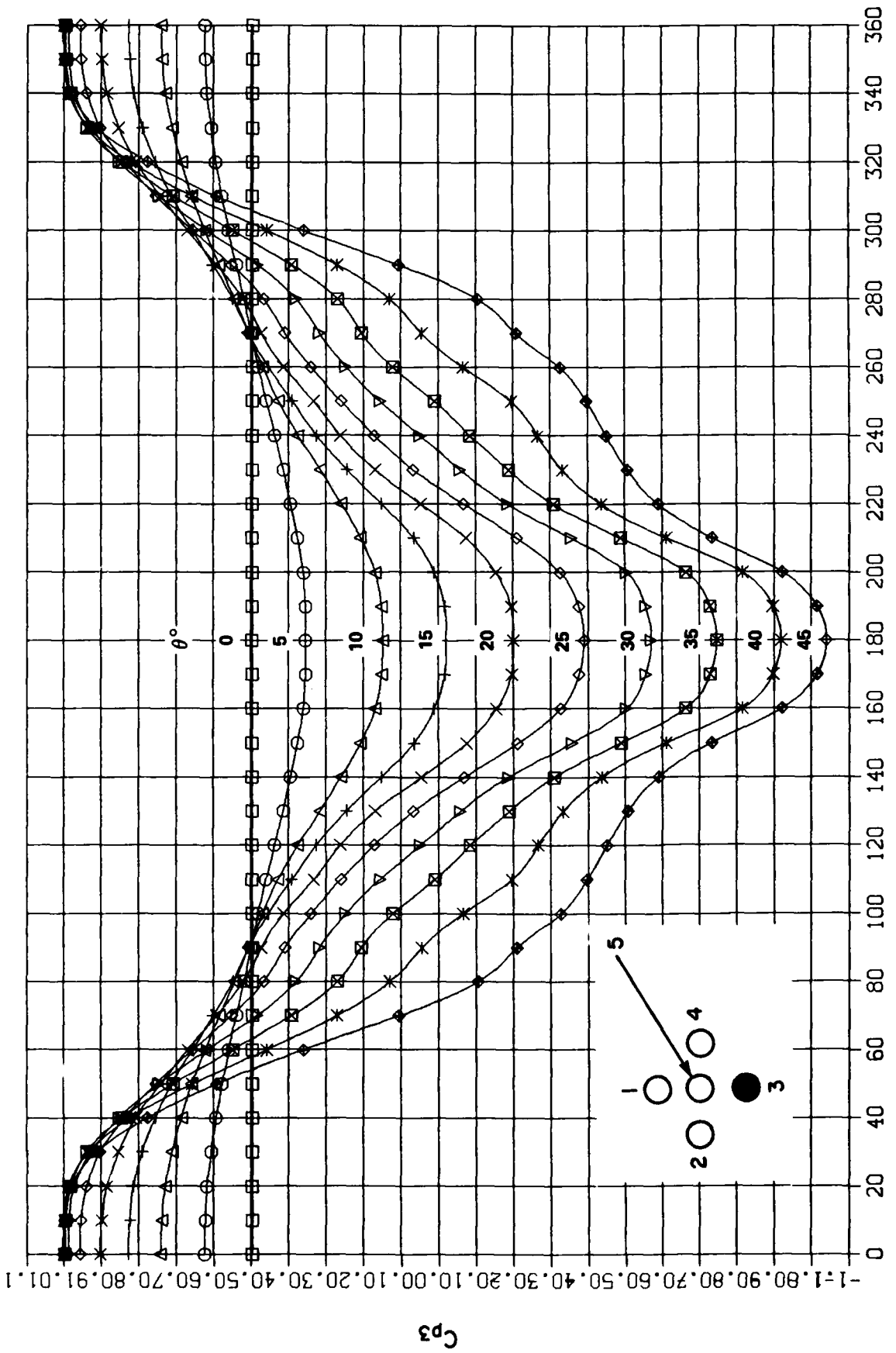

FIG. A8: PROBE SIDE ORIFICE PRESSURE COEFFICIENT, C_{p3}

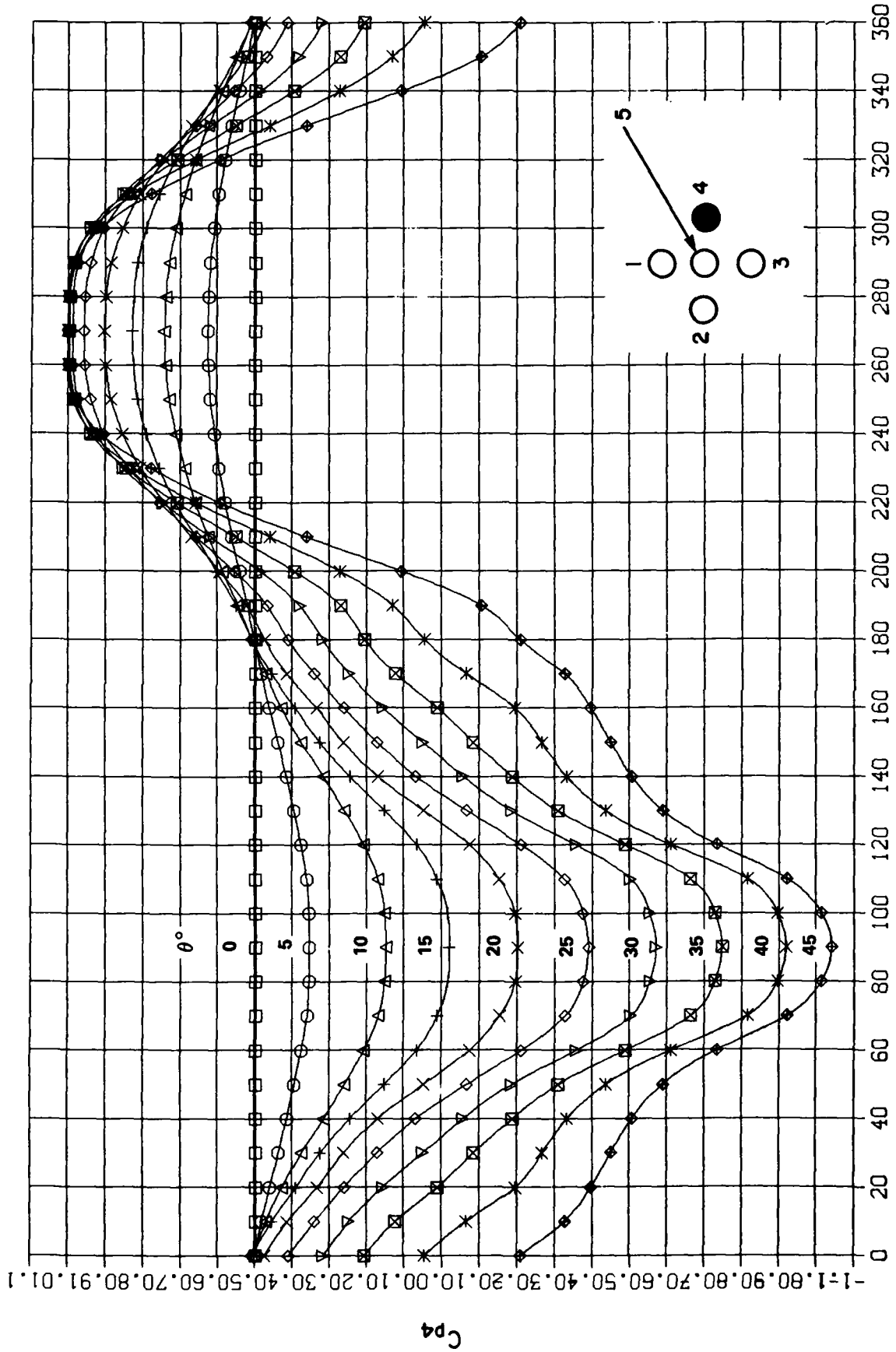

FIG. A9: PROBE SIDE ORIFICE PRESSURE COEFFICIENT, C_{p4}

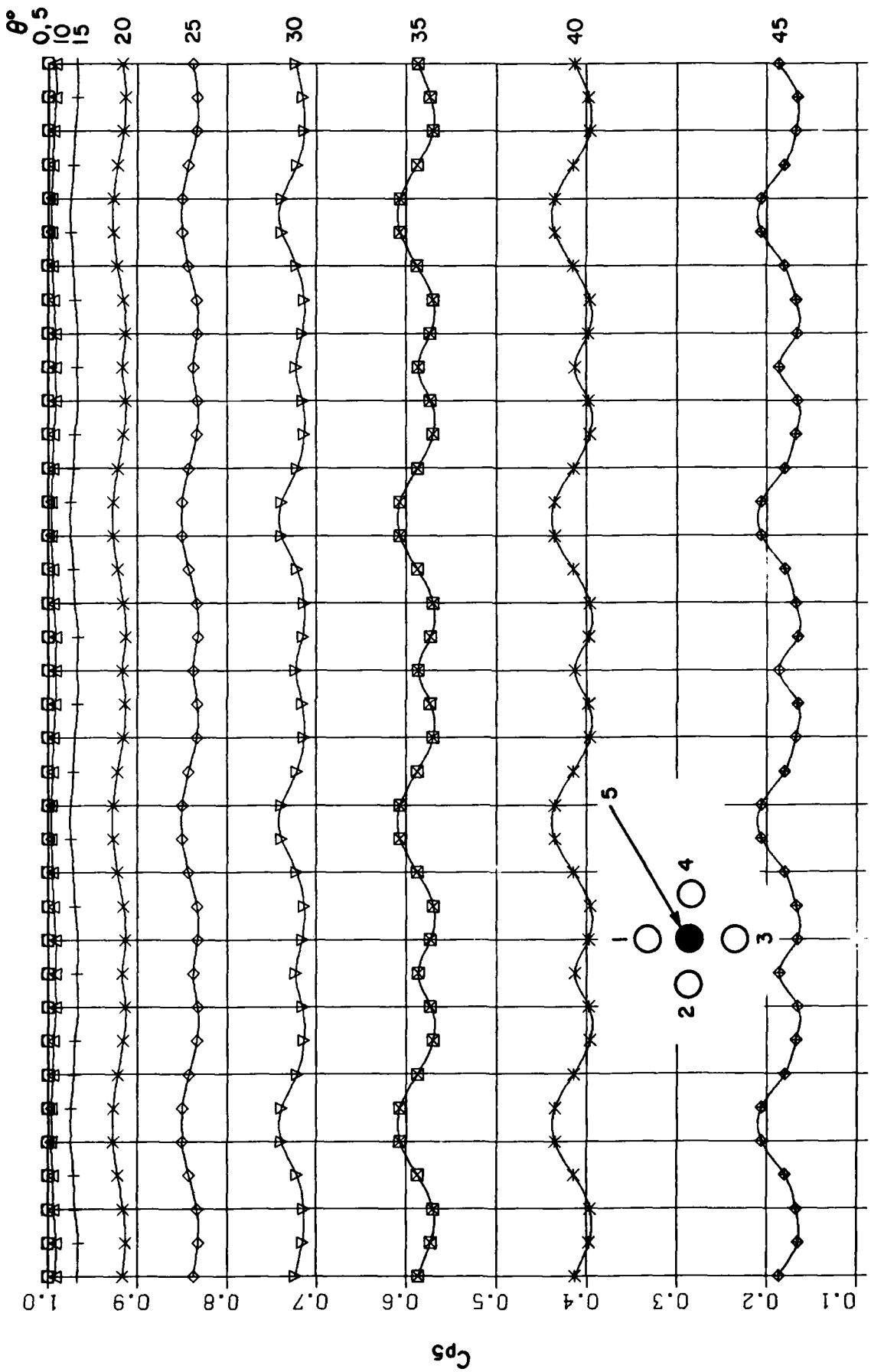

FIG. A10: PROBE CENTRAL ORIFICE PRESSURE COEFFICIENT, C_{p5}

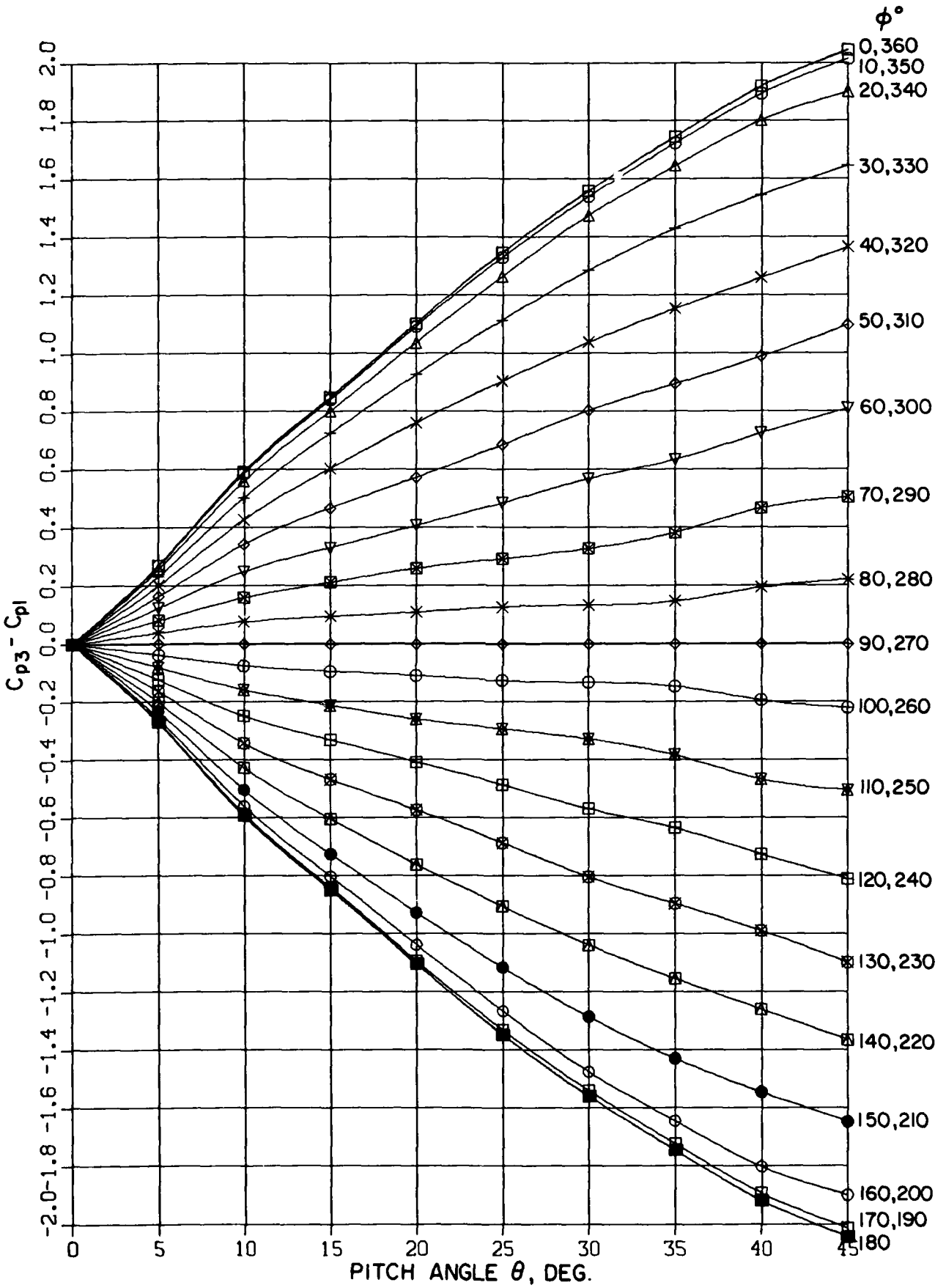

FIG. A11: PROBE ORIFICE PRESSURE DIFFERENTIAL ($C_{p3} - C_{p1}$) – UPWASH

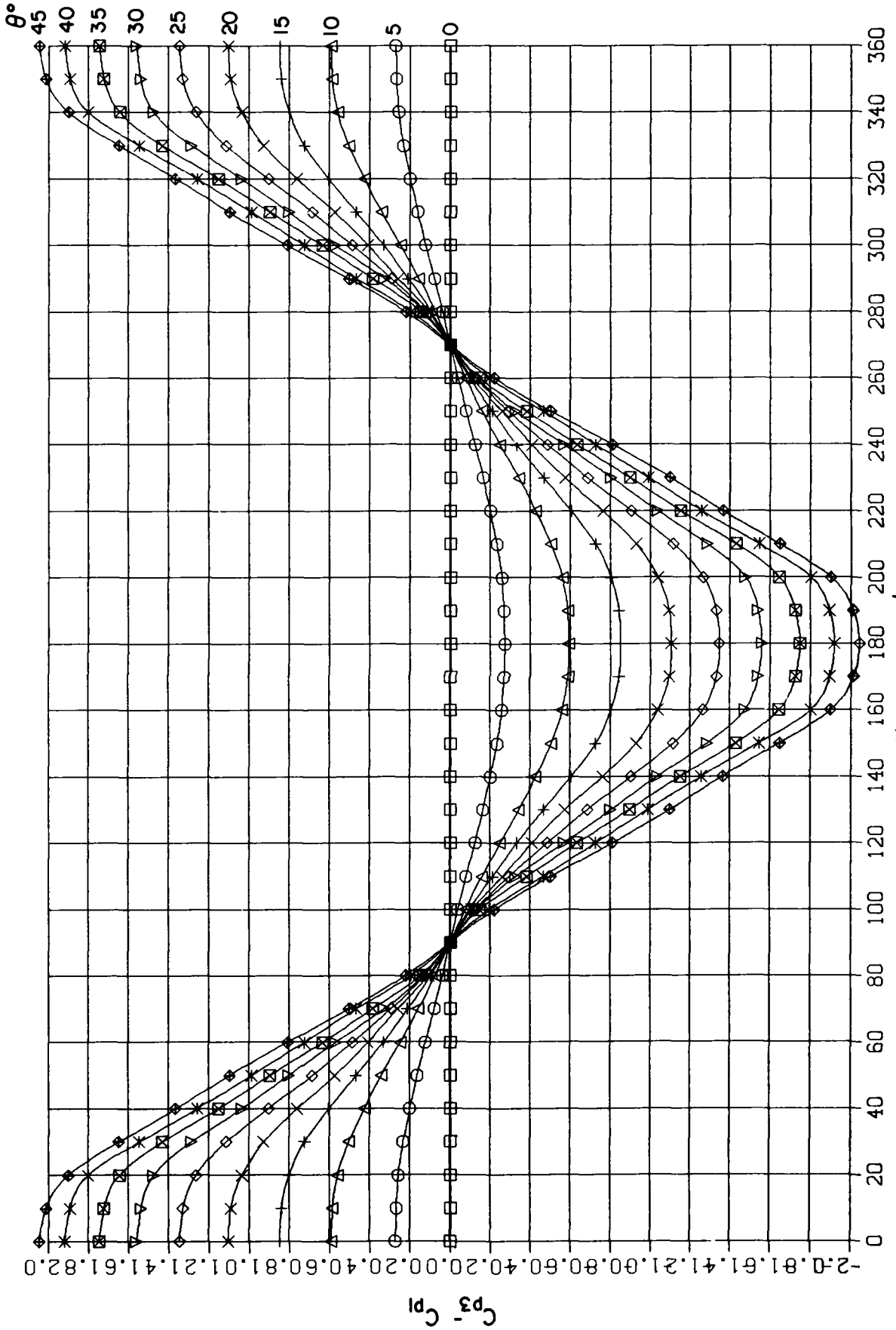

FIG. A12: PROBE ORIFICE PRESSURE DIFFERENTIAL ($C_{p3} - C_{p1}$) – UPWASH

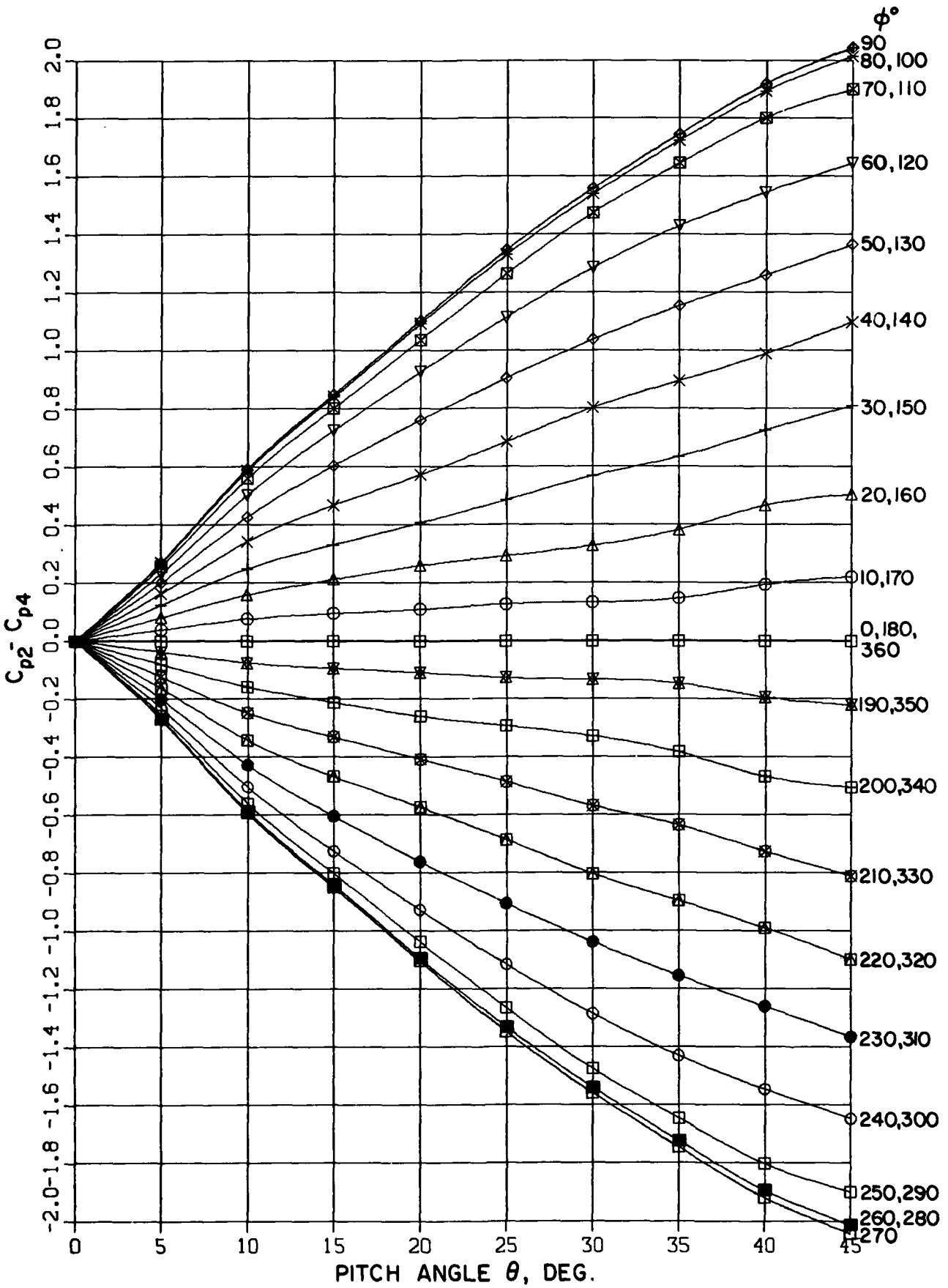

FIG. A13: PROBE ORIFICE PRESSURE DIFFERENTIAL ($C_{p2} - C_{p4}$) – DOWNWASH

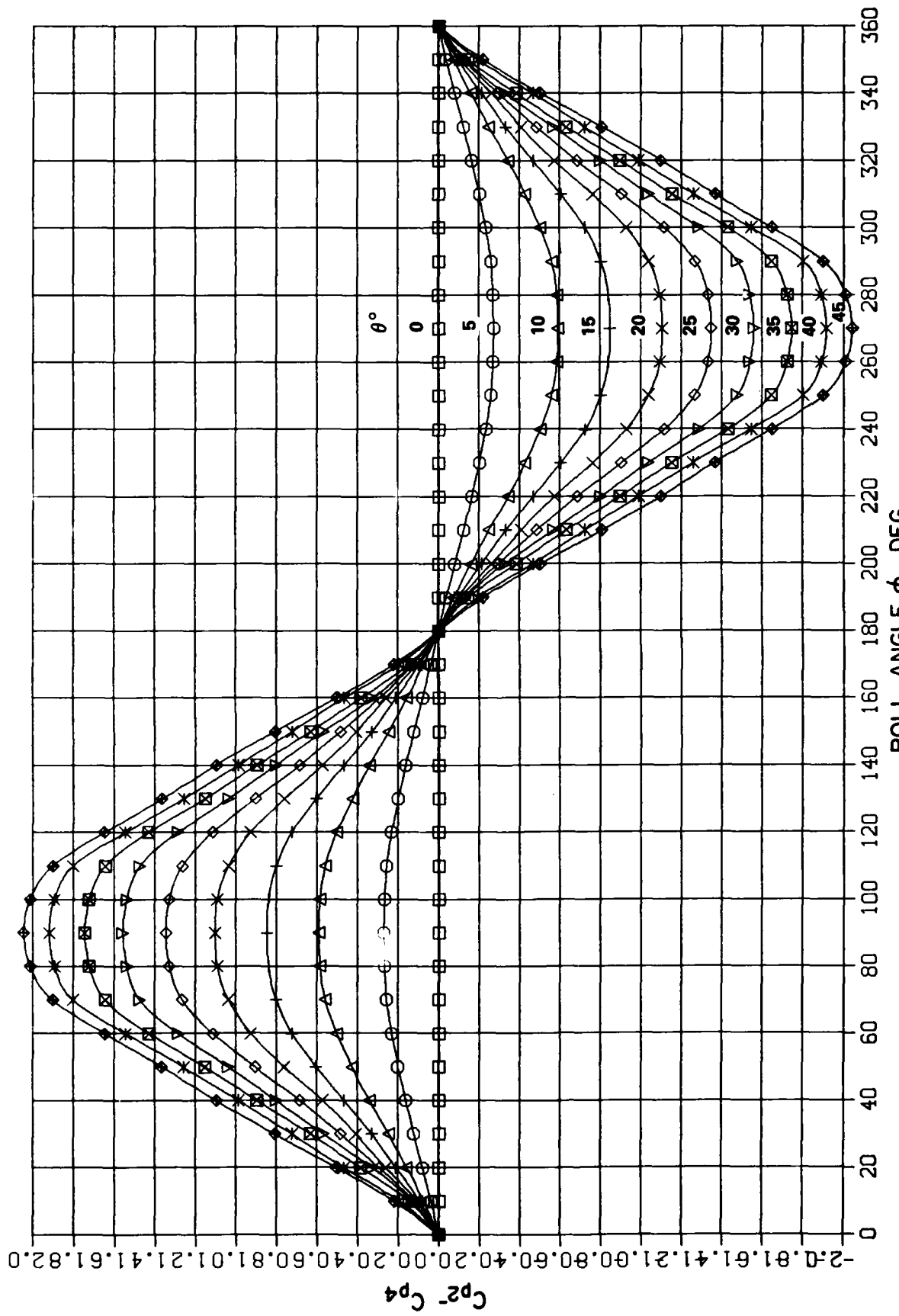

FIG. A14: PROBE ORIFICE PRESSURE DIFFERENTIAL ($C_{p2} - C_{p4}$) – DOWNWASH

APPENDIX B

TABULATION OF PROBE ORIFICE PRESSURE COEFFICIENTS, DERIVED FROM CALIBRATION DATA

PITCH ANGLE THETA	ROLL ANGLE, PHI 0.	10.	20.	30.	40.	50.	60.	70.	80.	90.
0.	0.496	0.496	0.496	0.496	0.496	0.496	0.496	0.496	0.496	0.496
5.	0.354	0.355	0.361	0.375	0.394	0.415	0.437	0.460	0.481	0.501
10.	0.148	0.151	0.169	0.207	0.259	0.316	0.375	0.428	0.470	0.508
15.	-0.021	-0.017	0.012	0.065	0.152	0.245	0.326	0.390	0.455	0.508
20.	-0.201	-0.195	-0.153	-0.074	0.047	0.169	0.262	0.333	0.414	0.473
25.	-0.390	-0.376	-0.327	-0.212	-0.067	0.068	0.171	0.260	0.340	0.411
30.	-0.571	-0.554	-0.503	-0.359	-0.186	-0.058	0.049	0.156	0.247	0.317
35.	-0.748	-0.728	-0.663	-0.490	-0.309	-0.188	-0.085	0.010	0.122	0.205
40.	-0.919	-0.896	-0.815	-0.611	-0.437	-0.332	-0.268	-0.196	-0.064	0.045
45.	-1.041	-1.014	-0.922	-0.734	-0.589	-0.506	-0.450	-0.397	-0.326	-0.209

PITCH ANGLE THETA	ROLL ANGLE, PHI 100.	110.	120.	130.	140.	150.	160.	170.	180.	190.
0.	0.496	0.496	0.496	0.496	0.496	0.496	0.496	0.496	0.496	0.496
5.	0.519	0.540	0.560	0.578	0.594	0.607	0.618	0.623	0.625	0.623
10.	0.545	0.586	0.624	0.659	0.687	0.710	0.729	0.738	0.741	0.738
15.	0.550	0.602	0.657	0.712	0.756	0.791	0.813	0.824	0.828	0.824
20.	0.522	0.593	0.670	0.742	0.809	0.853	0.884	0.899	0.902	0.899
25.	0.467	0.553	0.656	0.753	0.838	0.903	0.938	0.954	0.956	0.954
30.	0.380	0.485	0.617	0.746	0.852	0.927	0.972	0.986	0.988	0.986
35.	0.269	0.393	0.550	0.707	0.845	0.939	0.982	0.996	0.998	0.996
40.	0.129	0.271	0.458	0.656	0.823	0.935	0.987	0.998	1.000	0.998
45.	-0.106	0.108	0.360	0.592	0.776	0.913	0.978	1.000	1.001	1.000

PITCH ANGLE THETA	ROLL ANGLE, PHI 200.	210.	220.	230.	240.	250.	260.	270.	280.	290.
0.	0.496	0.496	0.496	0.496	0.496	0.496	0.496	0.496	0.496	0.496
5.	0.618	0.607	0.594	0.578	0.560	0.540	0.519	0.501	0.481	0.460
10.	0.729	0.710	0.687	0.659	0.624	0.586	0.545	0.508	0.470	0.428
15.	0.813	0.791	0.756	0.712	0.657	0.602	0.550	0.508	0.455	0.390
20.	0.884	0.853	0.809	0.742	0.670	0.593	0.522	0.473	0.414	0.333
25.	0.938	0.903	0.838	0.753	0.656	0.553	0.467	0.411	0.340	0.260
30.	0.972	0.927	0.852	0.746	0.617	0.485	0.380	0.317	0.247	0.156
35.	0.982	0.939	0.845	0.707	0.550	0.393	0.269	0.205	0.122	0.010
40.	0.987	0.935	0.823	0.656	0.458	0.271	0.129	0.045	-0.064	-0.196
45.	0.978	0.913	0.776	0.592	0.360	0.108	-0.106	-0.209	-0.326	-0.397

PITCH ANGLE THETA	ROLL ANGLE, PHI 300.	310.	320.	330.	340.	350.	360.
0.	0.496	0.496	0.496	0.496	0.496	0.496	0.496
5.	0.437	0.415	0.394	0.375	0.361	0.355	0.354
10.	0.375	0.316	0.259	0.207	0.169	0.151	0.148
15.	0.326	0.245	0.152	0.065	0.012	-0.017	-0.021
20.	0.262	0.169	0.047	-0.074	-0.153	-0.195	-0.201
25.	0.171	0.068	-0.067	-0.212	-0.327	-0.376	-0.390
30.	0.049	-0.058	-0.186	-0.359	-0.503	-0.554	-0.571
35.	-0.085	-0.188	-0.309	-0.490	-0.663	-0.728	-0.748
40.	-0.268	-0.332	-0.437	-0.611	-0.815	-0.896	-0.919
45.	-0.450	-0.506	-0.589	-0.734	-0.922	-1.014	-1.041

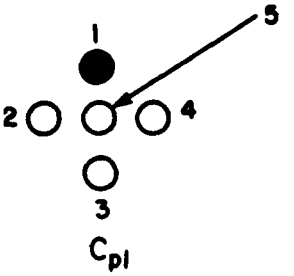

PITCH ANGLE THETA	ROLL ANGLE, PHI 0.	10.	20.	30.	40.	50.	60.	70.	80.	90.
0.	0.496	0.496	0.496	0.496	0.496	0.496	0.496	0.496	0.496	0.496
5.	0.501	0.519	0.540	0.560	0.578	0.594	0.607	0.618	0.623	0.625
10.	0.508	0.545	0.586	0.624	0.659	0.687	0.710	0.729	0.738	0.741
15.	0.508	0.550	0.602	0.657	0.712	0.756	0.791	0.813	0.824	0.828
20.	0.473	0.522	0.593	0.670	0.742	0.809	0.853	0.884	0.899	0.902
25.	0.411	0.467	0.553	0.656	0.753	0.838	0.903	0.938	0.954	0.956
30.	0.317	0.380	0.485	0.617	0.746	0.852	0.927	0.972	0.986	0.988
35.	0.205	0.269	0.393	0.550	0.707	0.845	0.939	0.982	0.996	0.998
40.	0.045	0.129	0.271	0.458	0.656	0.823	0.935	0.987	0.998	1.000
45.	-0.209	-0.106	0.108	0.360	0.592	0.776	0.913	0.978	1.000	1.001

PITCH ANGLE THETA	ROLL ANGLE, PHI 100.	110.	120.	130.	140.	150.	160.	170.	180.	190.
0.	0.496	0.496	0.496	0.496	0.496	0.496	0.496	0.496	0.496	0.496
5.	0.623	0.618	0.607	0.594	0.578	0.560	0.540	0.519	0.501	0.481
10.	0.738	0.729	0.710	0.687	0.659	0.624	0.586	0.545	0.508	0.470
15.	0.824	0.813	0.791	0.756	0.712	0.657	0.602	0.550	0.508	0.455
20.	0.899	0.884	0.853	0.809	0.742	0.670	0.593	0.522	0.473	0.414
25.	0.954	0.938	0.903	0.838	0.753	0.656	0.553	0.467	0.411	0.340
30.	0.986	0.972	0.927	0.852	0.746	0.617	0.485	0.380	0.317	0.247
35.	0.996	0.982	0.939	0.845	0.707	0.550	0.393	0.269	0.205	0.122
40.	0.998	0.987	0.935	0.823	0.656	0.458	0.271	0.129	0.045	-0.064
45.	1.000	0.978	0.913	0.776	0.592	0.360	0.108	-0.106	-0.209	-0.326

PITCH ANGLE THETA	ROLL ANGLE, PHI 200.	210.	220.	230.	240.	250.	260.	270.	280.	290.
0.	0.496	0.496	0.496	0.496	0.496	0.496	0.496	0.496	0.496	0.496
5.	0.460	0.437	0.415	0.394	0.375	0.361	0.355	0.354	0.355	0.361
10.	0.428	0.375	0.316	0.259	0.207	0.169	0.151	0.148	0.151	0.169
15.	0.390	0.326	0.245	0.152	0.065	0.012	-0.017	-0.021	-0.017	0.012
20.	0.333	0.262	0.169	0.047	-0.074	-0.153	-0.195	-0.201	-0.195	-0.153
25.	0.260	0.171	0.068	-0.067	-0.212	-0.327	-0.376	-0.390	-0.376	-0.327
30.	0.156	0.049	-0.058	-0.186	-0.359	-0.503	-0.554	-0.571	-0.554	-0.503
35.	0.010	-0.085	-0.188	-0.309	-0.490	-0.663	-0.728	-0.748	-0.728	-0.663
40.	-0.196	-0.268	-0.332	-0.437	-0.611	-0.815	-0.896	-0.919	-0.896	-0.815
45.	-0.397	-0.450	-0.506	-0.589	-0.734	-0.922	-1.014	-1.041	-1.014	-0.922

PITCH ANGLE THETA	ROLL ANGLE, PHI 300.	310.	320.	330.	340.	350.	360.
0.	0.496	0.496	0.496	0.496	0.496	0.496	0.496
5.	0.375	0.394	0.415	0.437	0.460	0.481	0.501
10.	0.207	0.259	0.316	0.375	0.428	0.470	0.508
15.	0.065	0.152	0.245	0.326	0.390	0.455	0.508
20.	-0.074	0.047	0.169	0.262	0.333	0.414	0.473
25.	-0.212	-0.067	0.068	0.171	0.260	0.340	0.411
30.	-0.359	-0.186	-0.058	0.049	0.156	0.247	0.317
35.	-0.490	-0.309	-0.188	-0.085	0.010	0.122	0.205
40.	-0.611	-0.437	-0.332	-0.268	-0.196	-0.064	0.045
45.	-0.734	-0.589	-0.506	-0.450	-0.397	-0.326	-0.209

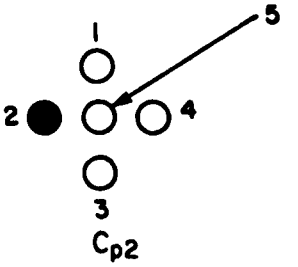

PITCH ANGLE THETA	ROLL ANGLE, PHI 0.	10.	20.	30.	40.	50.	60.	70.	80.	90.
0.	0.496	0.496	0.496	0.496	0.496	0.496	0.496	0.496	0.496	0.496
5.	0.625	0.623	0.618	0.607	0.594	0.578	0.560	0.540	0.519	0.501
10.	0.741	0.738	0.729	0.710	0.687	0.659	0.624	0.586	0.545	0.508
15.	0.828	0.824	0.813	0.791	0.756	0.712	0.657	0.602	0.550	0.508
20.	0.902	0.899	0.884	0.853	0.809	0.742	0.670	0.593	0.522	0.473
25.	0.956	0.954	0.938	0.903	0.838	0.753	0.656	0.553	0.467	0.411
30.	0.988	0.986	0.972	0.927	0.852	0.746	0.617	0.485	0.380	0.317
35.	0.998	0.996	0.982	0.939	0.845	0.707	0.550	0.393	0.269	0.205
40.	1.000	0.998	0.987	0.935	0.823	0.656	0.458	0.271	0.129	0.045
45.	1.001	1.000	0.978	0.913	0.776	0.592	0.360	0.108	-0.106	-0.209

PITCH ANGLE THETA	ROLL ANGLE, PHI 100.	110.	120.	130.	140.	150.	160.	170.	180.	190.
0.	0.496	0.496	0.496	0.496	0.496	0.496	0.496	0.496	0.496	0.496
5.	0.481	0.460	0.437	0.415	0.394	0.375	0.361	0.355	0.354	0.355
10.	0.470	0.428	0.375	0.316	0.259	0.207	0.169	0.151	0.148	0.151
15.	0.455	0.390	0.326	0.245	0.152	0.065	0.012	-0.017	-0.021	-0.017
20.	0.414	0.333	0.262	0.169	0.047	-0.074	-0.153	-0.195	-0.201	-0.195
25.	0.340	0.260	0.171	0.068	-0.067	-0.212	-0.327	-0.376	-0.390	-0.376
30.	0.247	0.156	0.049	-0.058	-0.186	-0.359	-0.503	-0.554	-0.571	-0.554
35.	0.122	0.010	-0.085	-0.188	-0.309	-0.490	-0.663	-0.728	-0.748	-0.728
40.	-0.064	-0.196	-0.268	-0.332	-0.437	-0.611	-0.815	-0.896	-0.919	-0.896
45.	-0.326	-0.397	-0.450	-0.506	-0.589	-0.734	-0.922	-1.014	-1.041	-1.014

PITCH ANGLE THETA	ROLL ANGLE, PHI 200.	210.	220.	230.	240.	250.	260.	270.	280.	290.
0.	0.496	0.496	0.496	0.496	0.496	0.496	0.496	0.496	0.496	0.496
5.	0.361	0.375	0.394	0.415	0.437	0.460	0.481	0.501	0.519	0.540
10.	0.169	0.207	0.259	0.316	0.375	0.428	0.470	0.508	0.545	0.586
15.	0.012	0.065	0.152	0.245	0.326	0.390	0.455	0.508	0.550	0.602
20.	-0.153	-0.074	0.047	0.169	0.262	0.333	0.414	0.473	0.522	0.593
25.	-0.327	-0.212	-0.067	0.068	0.171	0.260	0.340	0.411	0.467	0.553
30.	-0.503	-0.359	-0.186	-0.058	0.049	0.156	0.247	0.317	0.380	0.485
35.	-0.663	-0.490	-0.309	-0.188	-0.085	0.010	0.122	0.205	0.269	0.393
40.	-0.815	-0.611	-0.437	-0.332	-0.268	-0.196	-0.064	0.045	0.129	0.271
45.	-0.922	-0.734	-0.589	-0.506	-0.450	-0.397	-0.326	-0.209	-0.106	0.108

PITCH ANGLE THETA	ROLL ANGLE, PHI 300.	310.	320.	330.	340.	350.	360.
0.	0.496	0.496	0.496	0.496	0.496	0.496	0.496
5.	0.560	0.578	0.594	0.607	0.618	0.623	0.625
10.	0.624	0.659	0.687	0.710	0.729	0.738	0.741
15.	0.657	0.712	0.756	0.791	0.813	0.824	0.828
20.	0.670	0.742	0.809	0.853	0.884	0.899	0.902
25.	0.656	0.753	0.838	0.903	0.938	0.954	0.956
30.	0.617	0.746	0.852	0.927	0.972	0.986	0.988
35.	0.550	0.707	0.845	0.939	0.982	0.996	0.998
40.	0.458	0.656	0.823	0.935	0.987	0.998	1.000
45.	0.360	0.592	0.776	0.913	0.978	1.000	1.001

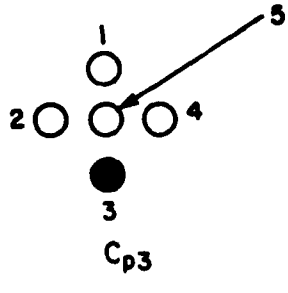

PITCH ANGLE THETA	ROLL ANGLE, PHI 0.	10.	20.	30.	40.	50.	60.	70.	80.	90.
0.	0.496	0.496	0.496	0.496	0.496	0.496	0.496	0.496	0.496	0.496
5.	0.501	0.481	0.460	0.437	0.415	0.394	0.375	0.361	0.355	0.354
10.	0.508	0.470	0.428	0.375	0.316	0.259	0.207	0.169	0.151	0.148
15.	0.506	0.455	0.390	0.326	0.245	0.152	0.065	0.012	-0.017	-0.021
20.	0.473	0.414	0.333	0.262	0.169	0.047	-0.074	-0.153	-0.195	-0.201
25.	0.411	0.340	0.260	0.171	0.068	-0.067	-0.212	-0.327	-0.376	-0.390
30.	0.317	0.247	0.156	0.049	-0.058	-0.186	-0.359	-0.503	-0.554	-0.571
35.	0.205	0.122	0.010	-0.085	-0.188	-0.309	-0.490	-0.663	-0.728	-0.748
40.	0.045	-0.064	-0.196	-0.268	-0.332	-0.437	-0.611	-0.815	-0.896	-0.919
45.	-0.209	-0.326	-0.397	-0.450	-0.506	-0.589	-0.734	-0.922	-1.014	-1.041

PITCH ANGLE THETA	ROLL ANGLE, PHI 100.	110.	120.	130.	140.	150.	160.	170.	180.	190.
0.	0.496	0.496	0.496	0.496	0.496	0.496	0.496	0.496	0.496	0.496
5.	0.355	0.361	0.375	0.394	0.415	0.437	0.460	0.481	0.501	0.519
10.	0.151	0.169	0.207	0.259	0.316	0.375	0.428	0.470	0.508	0.545
15.	-0.017	0.012	0.065	0.152	0.245	0.326	0.390	0.455	0.508	0.550
20.	-0.195	-0.153	-0.074	0.047	0.169	0.262	0.333	0.414	0.473	0.522
25.	-0.376	-0.327	-0.212	-0.067	0.068	0.171	0.260	0.340	0.411	0.467
30.	-0.554	-0.503	-0.359	-0.186	-0.058	0.049	0.156	0.247	0.317	0.380
35.	-0.728	-0.663	-0.490	-0.309	-0.188	-0.085	0.010	0.122	0.205	0.269
40.	-0.896	-0.815	-0.611	-0.457	-0.332	-0.268	-0.196	-0.064	0.045	0.129
45.	-1.014	-0.922	-0.734	-0.589	-0.506	-0.450	-0.397	-0.326	-0.209	-0.106

PITCH ANGLE THETA	ROLL ANGLE, PHI 200.	210.	220.	230.	240.	250.	260.	270.	280.	290.
0.	0.496	0.496	0.496	0.496	0.496	0.496	0.496	0.496	0.496	0.496
5.	0.540	0.560	0.578	0.594	0.607	0.618	0.623	0.625	0.623	0.618
10.	0.586	0.624	0.659	0.687	0.710	0.729	0.738	0.741	0.738	0.729
15.	0.602	0.657	0.712	0.756	0.791	0.813	0.824	0.828	0.824	0.813
20.	0.593	0.670	0.742	0.809	0.853	0.884	0.899	0.902	0.899	0.884
25.	0.553	0.656	0.753	0.838	0.903	0.938	0.954	0.956	0.954	0.938
30.	0.485	0.617	0.746	0.852	0.927	0.972	0.986	0.988	0.986	0.972
35.	0.393	0.550	0.707	0.845	0.939	0.982	0.996	0.998	0.996	0.982
40.	0.271	0.458	0.656	0.823	0.935	0.987	0.998	1.000	0.998	0.987
45.	0.108	0.360	0.592	0.776	0.913	0.978	1.000	1.001	1.000	0.978

PITCH ANGLE THETA	ROLL ANGLE, PHI 300.	310.	320.	330.	340.	350.	360.
0.	0.496	0.496	0.496	0.496	0.496	0.496	0.496
5.	0.607	0.594	0.578	0.560	0.540	0.519	0.501
10.	0.710	0.687	0.659	0.624	0.586	0.545	0.508
15.	0.791	0.756	0.712	0.657	0.602	0.550	0.508
20.	0.853	0.809	0.742	0.670	0.593	0.522	0.473
25.	0.903	0.838	0.753	0.656	0.553	0.467	0.411
30.	0.927	0.852	0.746	0.617	0.485	0.380	0.317
35.	0.939	0.845	0.707	0.550	0.393	0.269	0.205
40.	0.935	0.823	0.656	0.458	0.271	0.129	0.045
45.	0.913	0.776	0.592	0.360	0.108	-0.106	-0.209

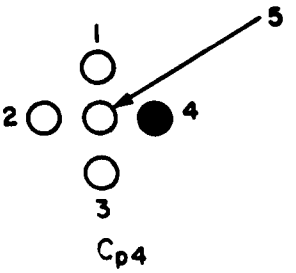

PITCH ANGLE THETA	ROLL ANGLE, PHI 0.	10.	20.	30.	40.	50.	60.	70.	80.	90.
0.	1.000	1.000	1.000	1.000	1.000	1.000	1.000	1.000	1.000	1.000
5.	0.999	0.999	0.999	0.999	0.999	0.999	0.999	0.999	0.999	0.999
10.	0.991	0.991	0.993	0.994	0.996	0.996	0.994	0.993	0.991	0.991
15.	0.967	0.966	0.970	0.971	0.974	0.974	0.971	0.970	0.966	0.967
20.	0.917	0.913	0.916	0.922	0.927	0.927	0.922	0.916	0.913	0.917
25.	0.838	0.833	0.834	0.843	0.850	0.850	0.843	0.834	0.833	0.838
30.	0.723	0.716	0.714	0.722	0.739	0.739	0.722	0.714	0.716	0.723
35.	0.587	0.573	0.570	0.588	0.607	0.607	0.588	0.570	0.573	0.587
40.	0.413	0.398	0.396	0.415	0.436	0.436	0.415	0.396	0.398	0.413
45.	0.187	0.166	0.168	0.180	0.206	0.206	0.180	0.168	0.166	0.187

PITCH ANGLE THETA	ROLL ANGLE, PHI 100.	110.	120.	130.	140.	150.	160.	170.	180.	190.
0.	1.000	1.000	1.000	1.000	1.000	1.000	1.000	1.000	1.000	1.000
5.	0.999	0.999	0.999	0.999	0.999	0.999	0.999	0.999	0.999	0.999
10.	0.991	0.993	0.994	0.996	0.996	0.994	0.993	0.991	0.991	0.991
15.	0.966	0.970	0.971	0.974	0.974	0.971	0.970	0.966	0.967	0.966
20.	0.913	0.916	0.922	0.927	0.927	0.922	0.916	0.913	0.917	0.913
25.	0.833	0.834	0.843	0.850	0.850	0.843	0.834	0.833	0.838	0.833
30.	0.716	0.714	0.722	0.739	0.739	0.722	0.714	0.716	0.723	0.716
35.	0.573	0.570	0.588	0.607	0.607	0.588	0.570	0.573	0.587	0.573
40.	0.398	0.396	0.415	0.436	0.436	0.415	0.396	0.398	0.413	0.398
45.	0.166	0.168	0.180	0.206	0.206	0.180	0.168	0.166	0.187	0.166

PITCH ANGLE THETA	ROLL ANGLE, PHI 200.	210.	220.	230.	240.	250.	260.	270.	280.	290.
0.	1.000	1.000	1.000	1.000	1.000	1.000	1.000	1.000	1.000	1.000
5.	0.999	0.999	0.999	0.999	0.999	0.999	0.999	0.999	0.999	0.999
10.	0.993	0.994	0.996	0.996	0.994	0.993	0.991	0.991	0.991	0.993
15.	0.970	0.971	0.974	0.974	0.971	0.970	0.966	0.967	0.966	0.970
20.	0.916	0.922	0.927	0.927	0.922	0.916	0.913	0.917	0.913	0.916
25.	0.834	0.843	0.850	0.850	0.843	0.834	0.833	0.838	0.833	0.834
30.	0.714	0.722	0.739	0.739	0.722	0.714	0.716	0.723	0.716	0.714
35.	0.570	0.588	0.607	0.607	0.588	0.570	0.573	0.587	0.573	0.570
40.	0.396	0.415	0.436	0.436	0.415	0.396	0.398	0.413	0.398	0.396
45.	0.168	0.180	0.206	0.206	0.180	0.168	0.166	0.187	0.166	0.168

PITCH ANGLE THETA	ROLL ANGLE, PHI 300.	310.	320.	330.	340.	350.	360.
0.	1.000	1.000	1.000	1.000	1.000	1.000	1.000
5.	0.999	0.999	0.999	0.999	0.999	0.999	0.999
10.	0.994	0.996	0.996	0.994	0.993	0.991	0.991
15.	0.971	0.974	0.974	0.971	0.970	0.966	0.967
20.	0.922	0.927	0.927	0.922	0.916	0.913	0.917
25.	0.843	0.850	0.850	0.843	0.834	0.833	0.838
30.	0.722	0.739	0.739	0.722	0.714	0.716	0.723
35.	0.588	0.607	0.607	0.588	0.570	0.573	0.587
40.	0.415	0.436	0.436	0.415	0.396	0.398	0.413
45.	0.180	0.206	0.206	0.180	0.168	0.166	0.187

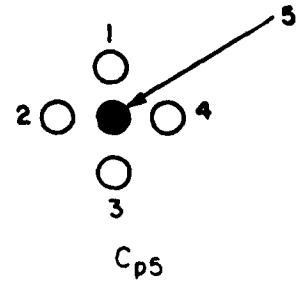

REPORT DOCUMENTATION PAGE / PAGE DE DOCUMENTATION DE RAPPORT

AD-A160262

REPORT/RAPPORT	REPORT/RAPPORT
NAE-AN-29 (1a)	NRC No. 24468 (1b)
REPORT SECURITY CLASSIFICATION / CLASSIFICATION DE SÉCURITÉ DE RAPPORT: Unclassified (2)	DISTRIBUTION (LIMITATIONS): Unlimited (3)

TITLE/SUBTITLE/TITRE/SOUS-TITRE (4)

Calibration and Use of Five-Hole Flow Direction Probes for Low Speed Wind Tunnel Application

AUTHOR(S)/AUTEUR(S) (5)

R.H. Wickens, C.D. Williams

SERIES/SÉRIE (6)

Aeronautical Note

CORPORATE AUTHOR/PERFORMING AGENCY/AUTEUR D'ENTREPRISE/AGENCE D'EXÉCUTION (7)

National Research Council Canada
National Aeronautical Establishment — Low Speed Aerodynamics Laboratory

SPONSORING AGENCY/AGENCE DE SUBVENTION (8)

DATE (9)	FILE/DOSSIER (10)	LAB. ORDER / COMMANDE DU LAB. (11)	PAGES (12a)	FIGS/DIAGRAMMES (12b)
85-07			49	6

NOTES (13)

DESCRIPTORS (KEY WORDS)/MOTS-CLÉS (14)

1. Wind tunnels — instrumentation

SUMMARY/SOMMAIRE (15)

This note describes a method of calibration and use of five-hole flow direction probes. When used in complex three-dimensional mixed flows, the probe will furnish flow directions, velocity components and total pressures. The method described in this note is intended for the use of the wind tunnel project engineer in determining flow direction characteristics of various model configurations.

END

FILMED

11-85

DTIC